

Circuit Quantum Electrodynamics

Superconducting platform (third Lecture)

Covering: basic concepts, measurement techniques,
implementations, qubit approaches, current trends

With figures and slides borrowed from
A. Wallraff (ETH-Zurich), P. Bertet (CEA Saclay)

Decoherence (Relaxation and Dephasing)

Source and mitigation of noise

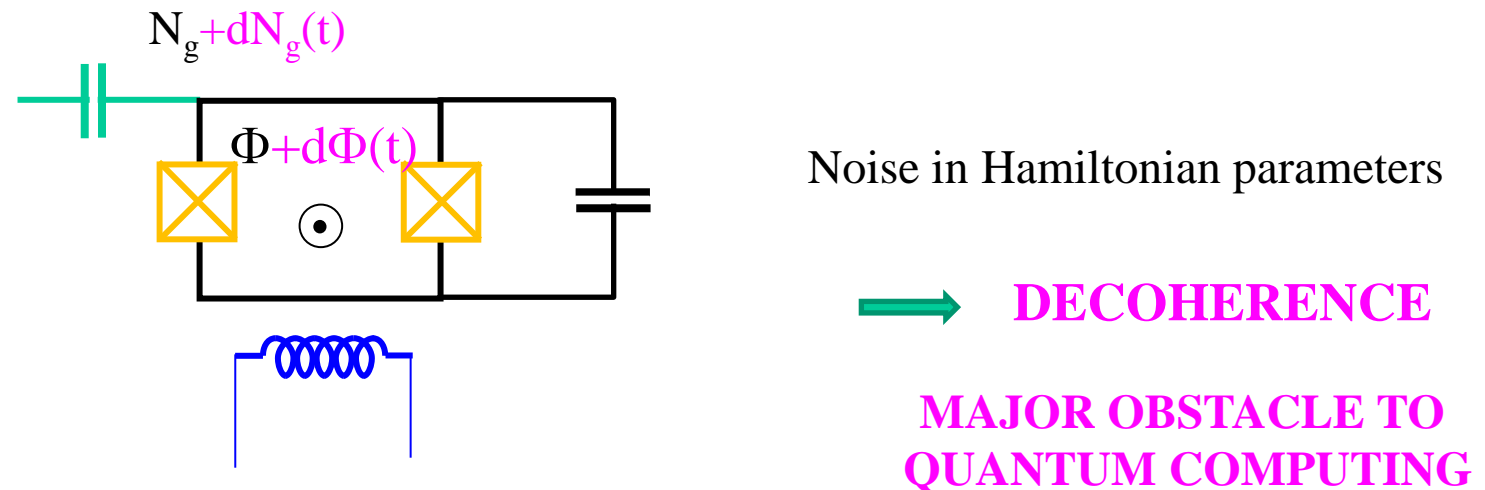
Relaxation mechanisms (T_1)

- 1) Radiative decay and ohmic loss due to coupling of the qubit to the electromagnetic environment.
- 2) Coupling to material defects described by two-level systems (TLS) mostly at the material interfaces
- 3) Relaxation induced by quasiparticle tunneling
- 4) Other sources, e.g. vortex dynamics.

Dephasing mechanisms (T_2)

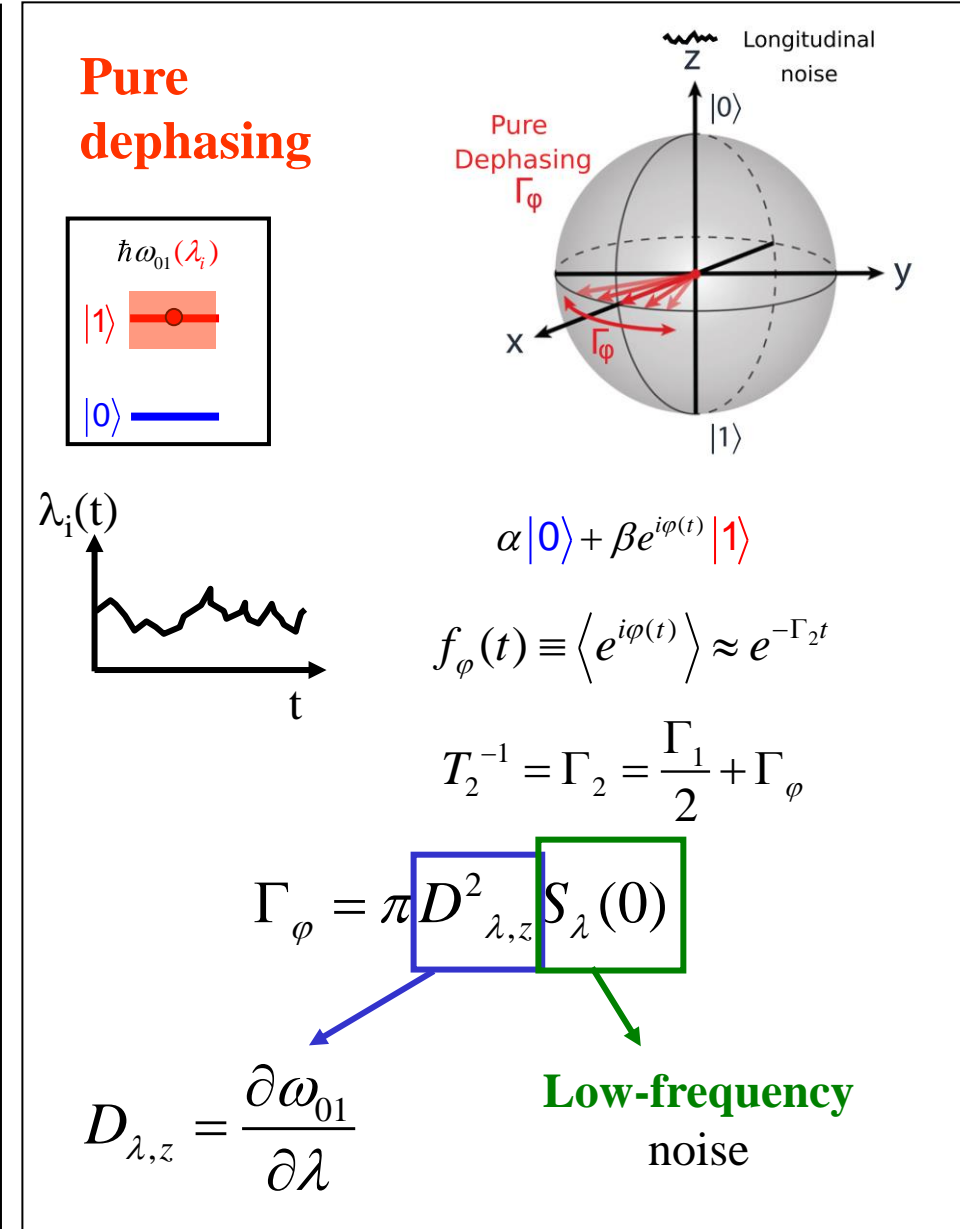
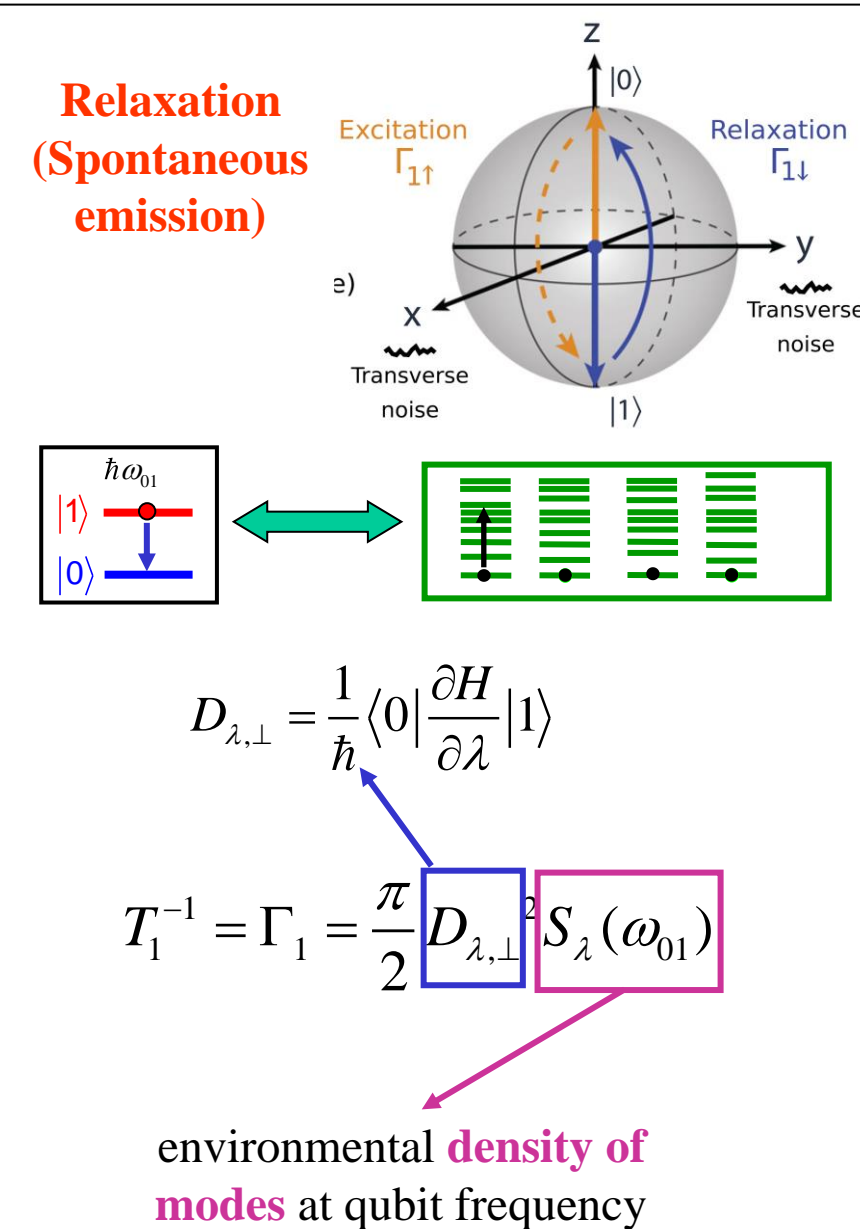
- 1) Photon shot noise through dispersively coupled elements, e.g. residual photons in the readout circuit.
- 2) Magnetic flux noise in flux-tunable qubits.
- 3) Charge noise in combination with charge dispersion of transmon energy levels.

Decoherence

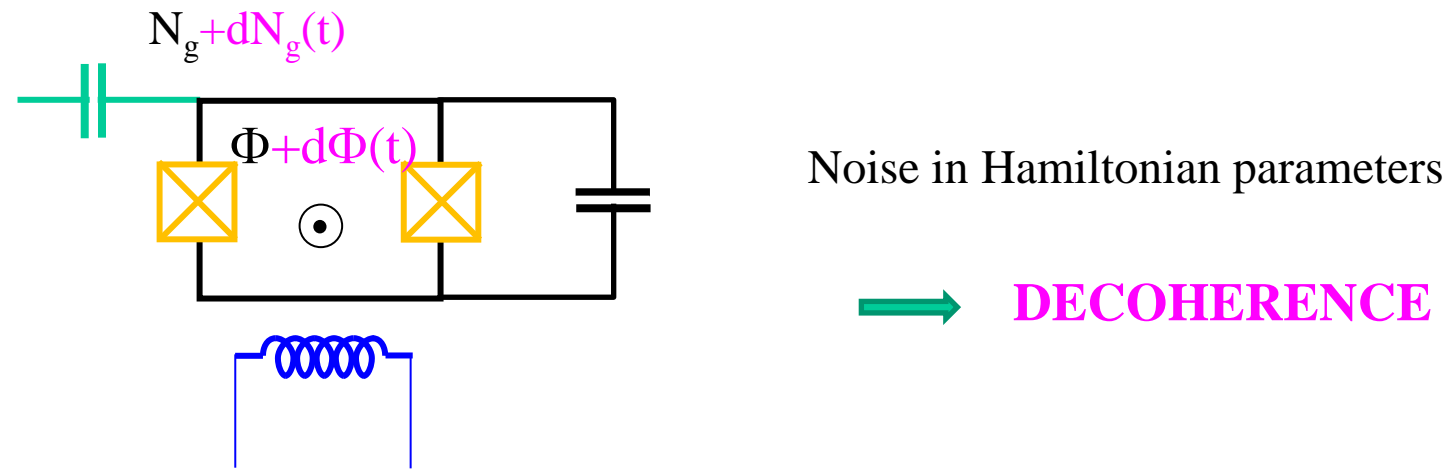


Decoherence in superconducting qubits

(Ithier et al., PRB 72, 134519, 2005)

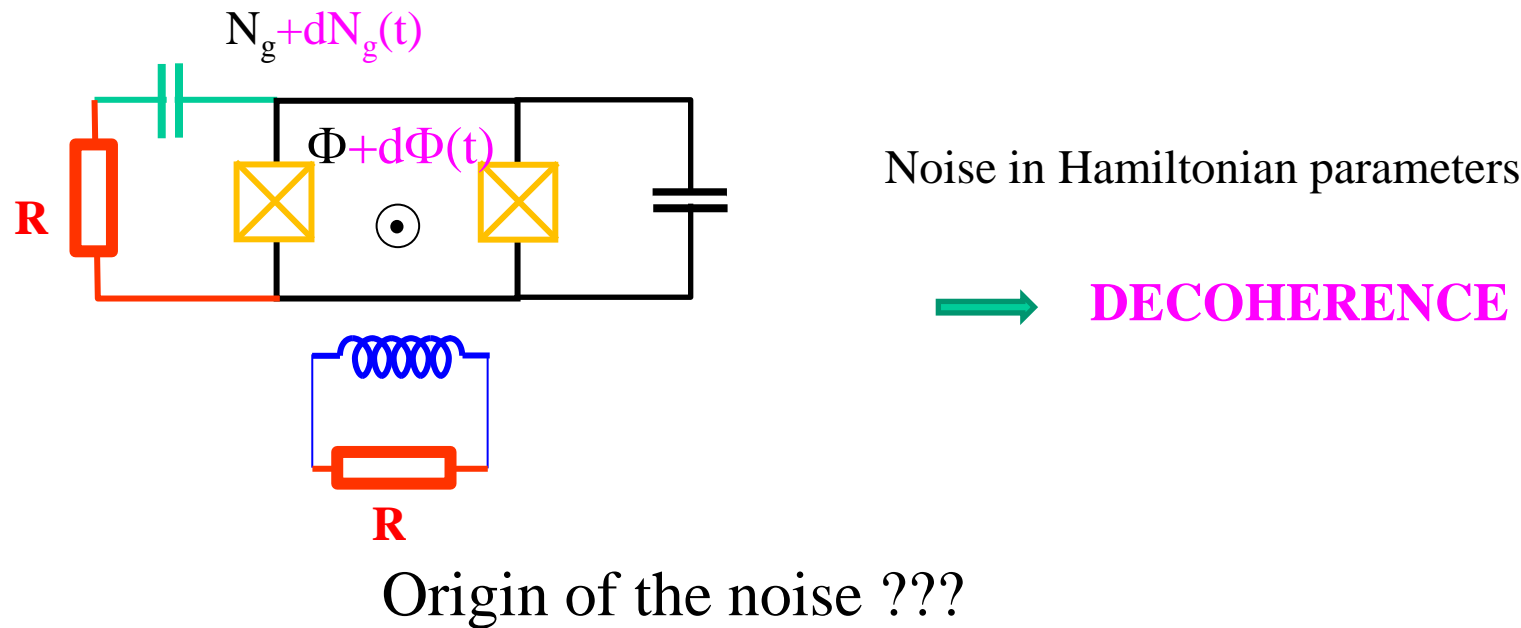


Decoherence



Origin of the noise ???

Decoherence

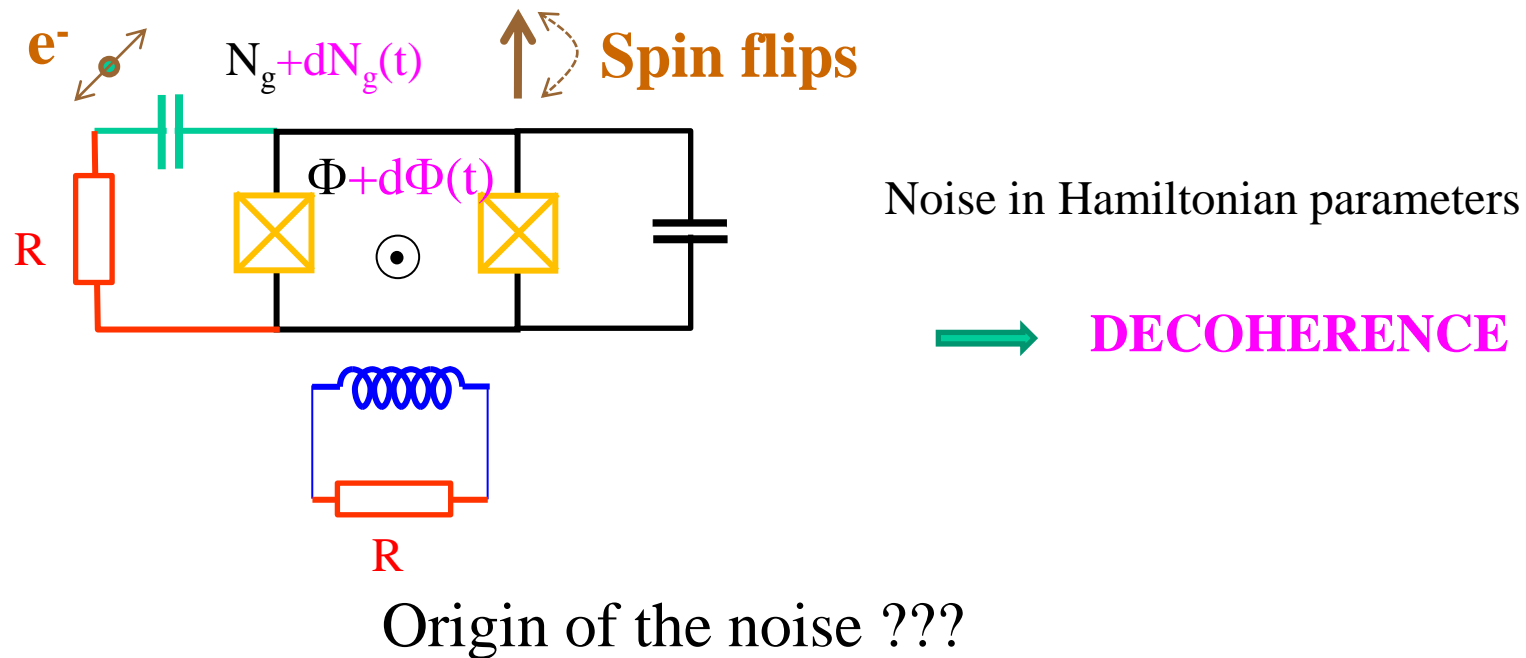


1) ELECTROMAGNETIC

- Low-frequency : Johnson-Nyquist due to thermal noise
- High-frequency : spontaneous emission (quantum noise)

≈ Under control

Decoherence



2) MICROSCOPIC

Low-frequency noise
well studied :

Charge noise

$$S_{Ng}(\omega) \sim \frac{(10^{-3})^2}{\omega}$$

Flux noise

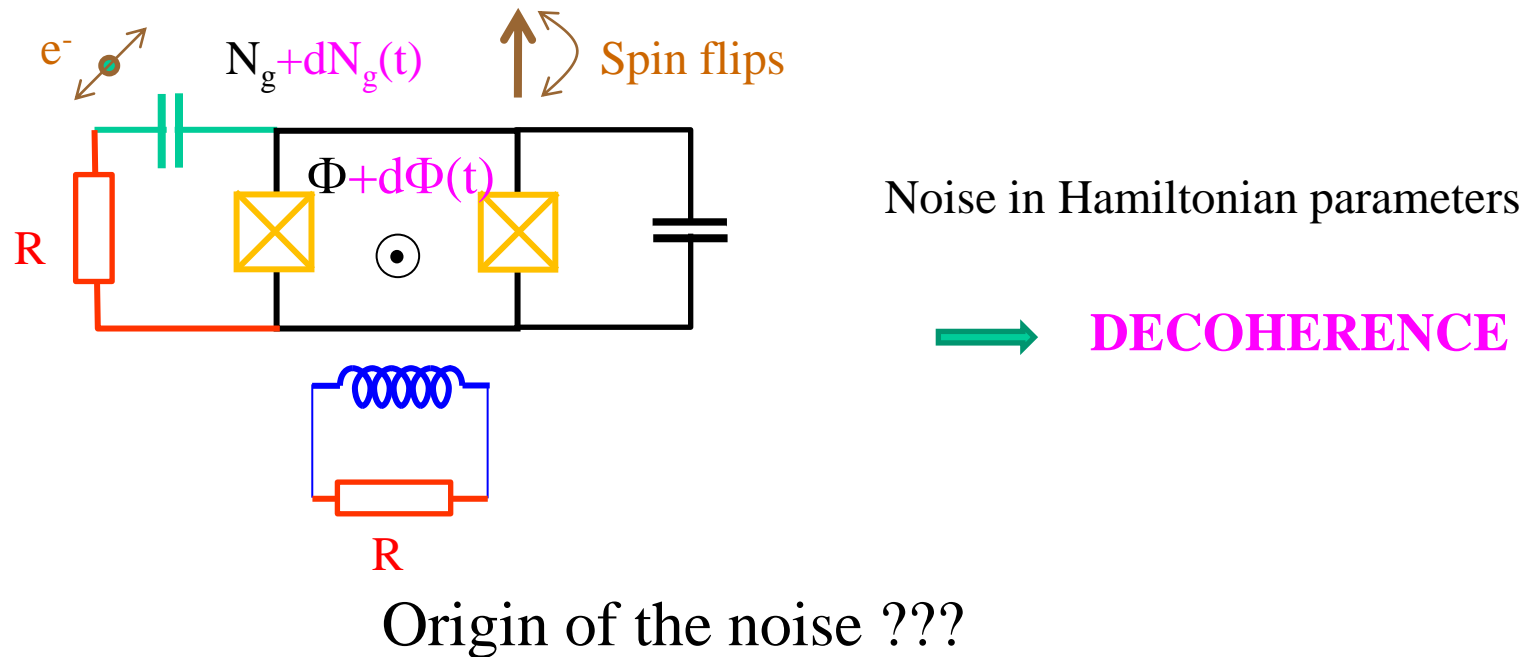
$$S_{\Phi}(\omega) \sim \frac{(10^{-6}\Phi_0)^2}{\omega}$$

High-frequency (GHz)
microscopic noise

DIFFICULT TO CONTROL !!

courtesy CEA Saclay

Decoherence



2) MICROSCOPIC

Low-frequency noise
well studied :

CPB in charge regime

Transmon

High-frequency (GHz)
microscopic noise

Charge noise

$$S_{Ng}(\omega) \sim \frac{(10^{-3})^2}{\omega}$$

$$T_2 \sim 10 - 100 \text{ ns}$$

$$T_2 \sim 1 - 10 \text{ ms}$$

Flux noise

$$S_{\Phi}(\omega) \sim \frac{(10^{-6} \Phi_0)^2}{\omega}$$

$$T_2 \sim 1 - 100 \mu\text{s}$$

$$T_2 \sim 1 - 100 \mu\text{s}$$

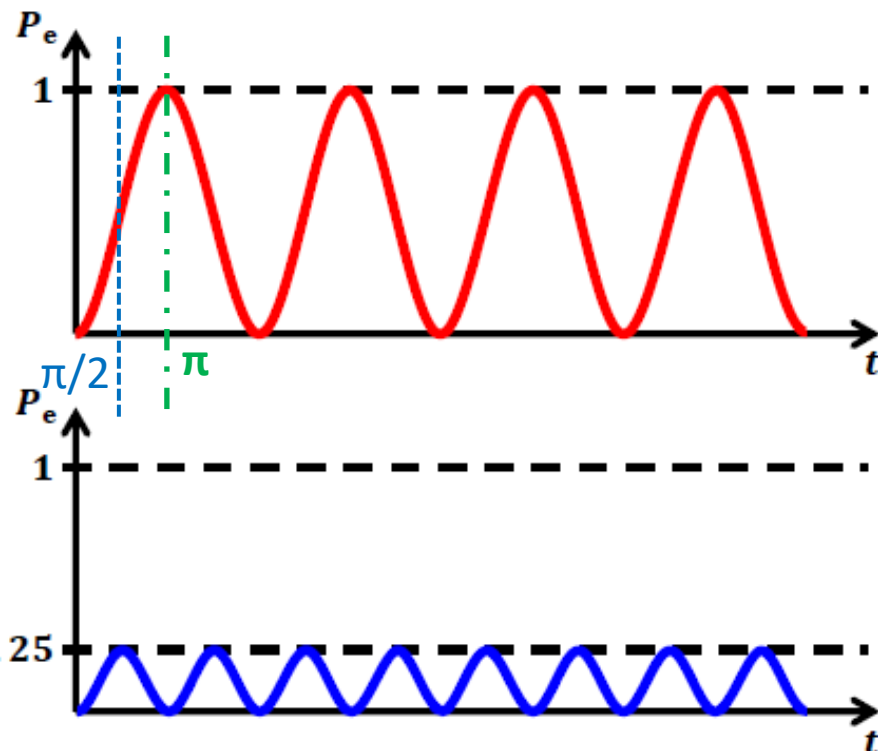
DIFFICULT TO CONTROL !!

courtesy CEA Saclay

Ideal Rabi Oscillations: no dissipation

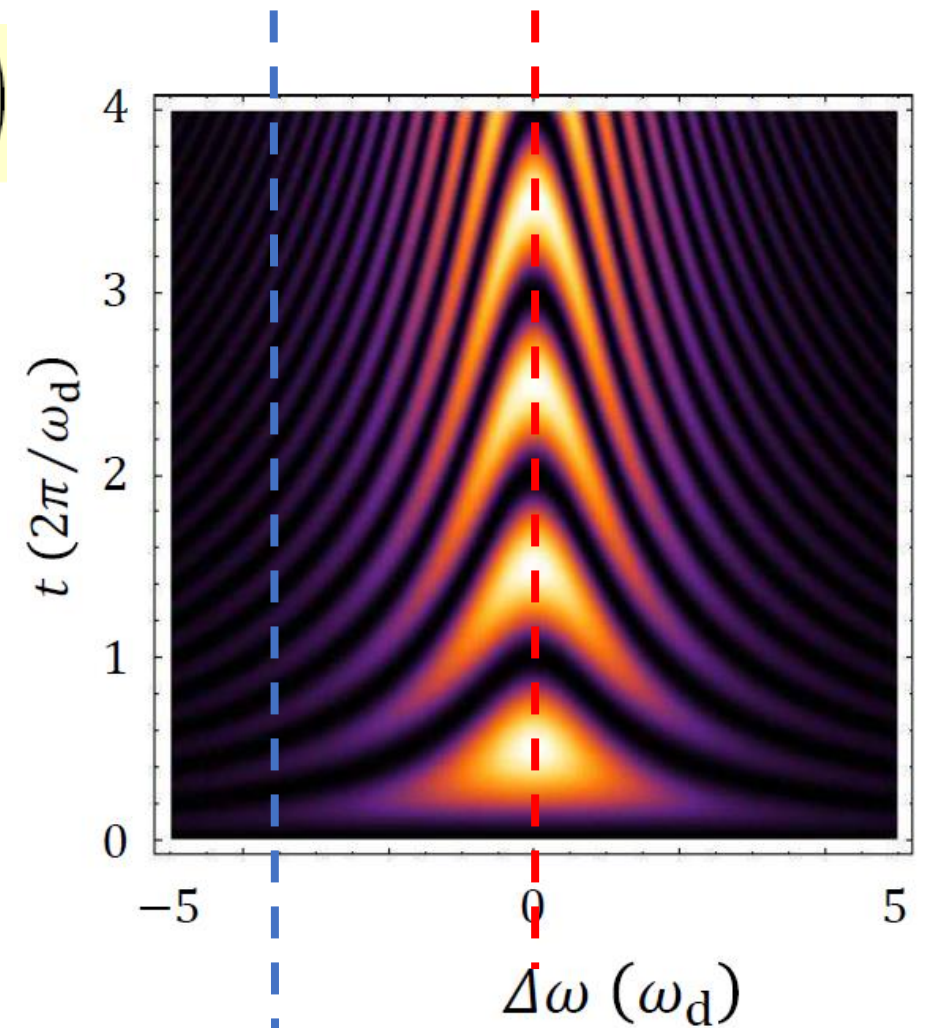
Rabi Oscillations – Graphical representation

On resonance $\omega = \omega_q$



Detuning $|\Delta\omega| = \sqrt{3} \omega_d$

$$P_e = \frac{\omega_d^2}{\Delta\omega^2 + \omega_d^2} \sin^2\left(\frac{t\sqrt{\Delta\omega^2 + \omega_d^2}}{2}\right)$$



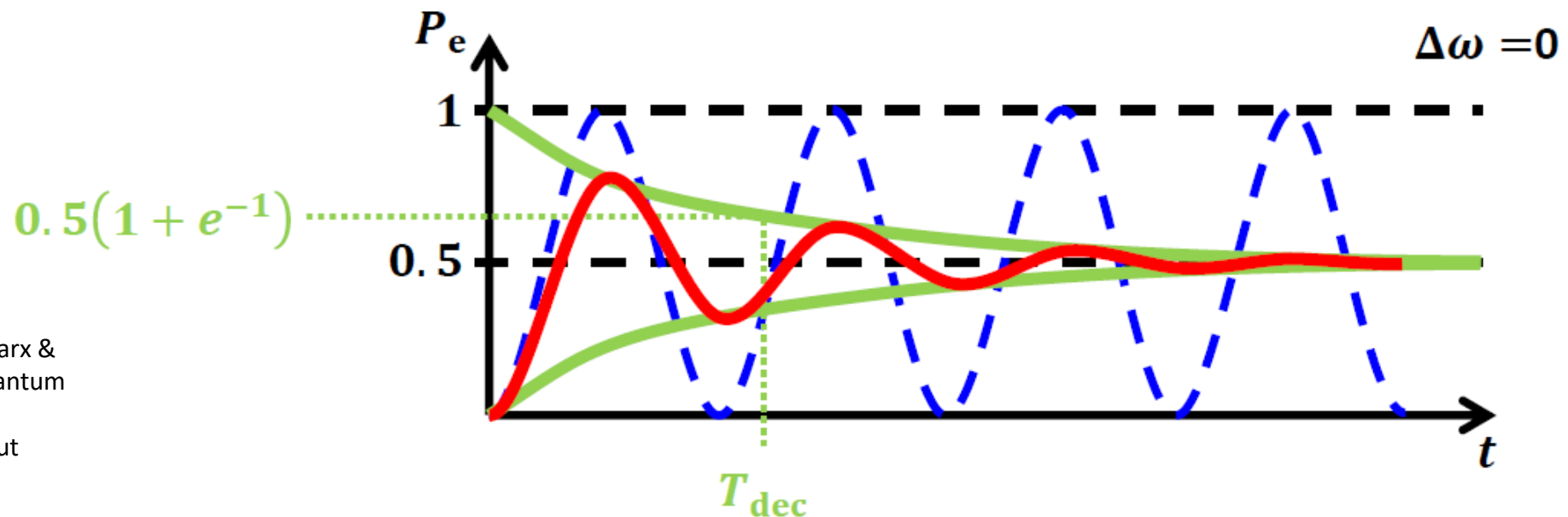
Real Rabi Oscillations: decay time

$$P_e = \frac{\omega_d^2}{\Delta\omega^2 + \omega_d^2} \sin^2\left(\frac{t\sqrt{\Delta\omega^2 + \omega_d^2}}{2}\right)$$

Complicated interplay between T_1 , T_2^* , and the drive

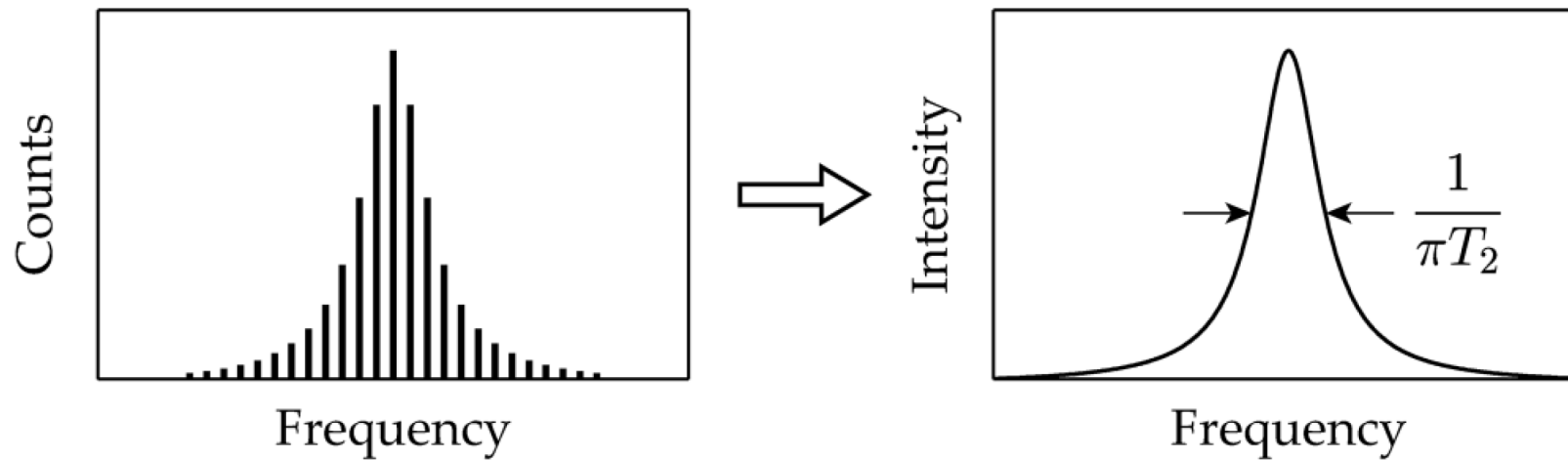
- At long times, small oscillations persist for oscillatory drive
- Nevertheless useful **order-of-magnitude check** for T_{dec}
- Important tool for single-qubit gates

- To determine T_1 , T_2^* , T_2 correctly, more sophisticated protocols are required
- Energy relaxation measurements, Ramsey fringes, spin echo

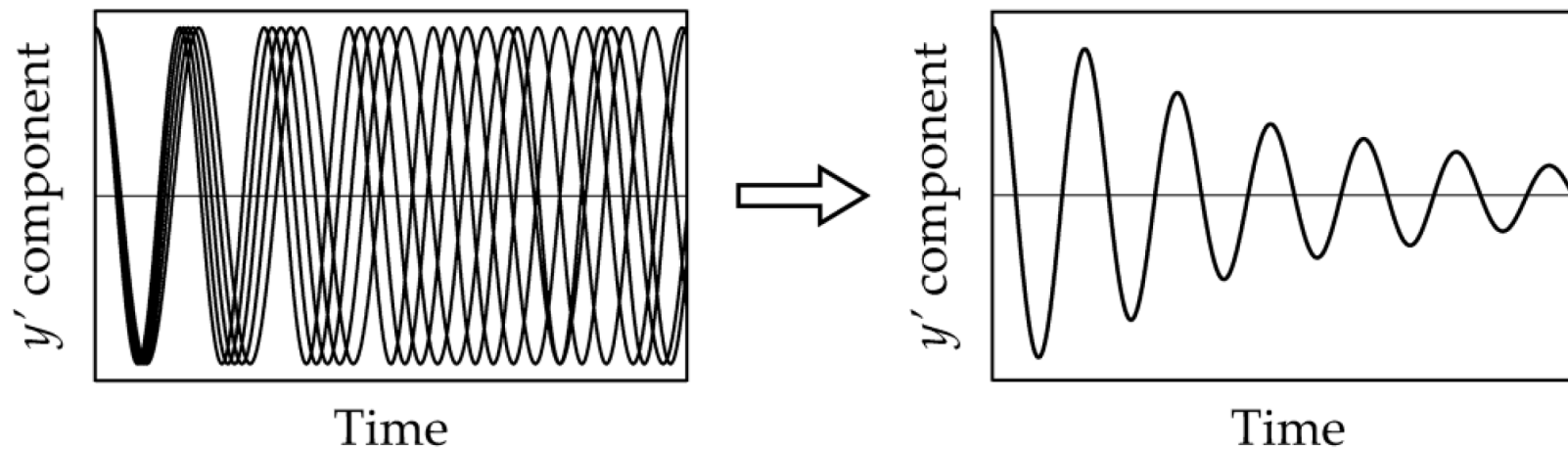


Intuitive understanding of Dephasing

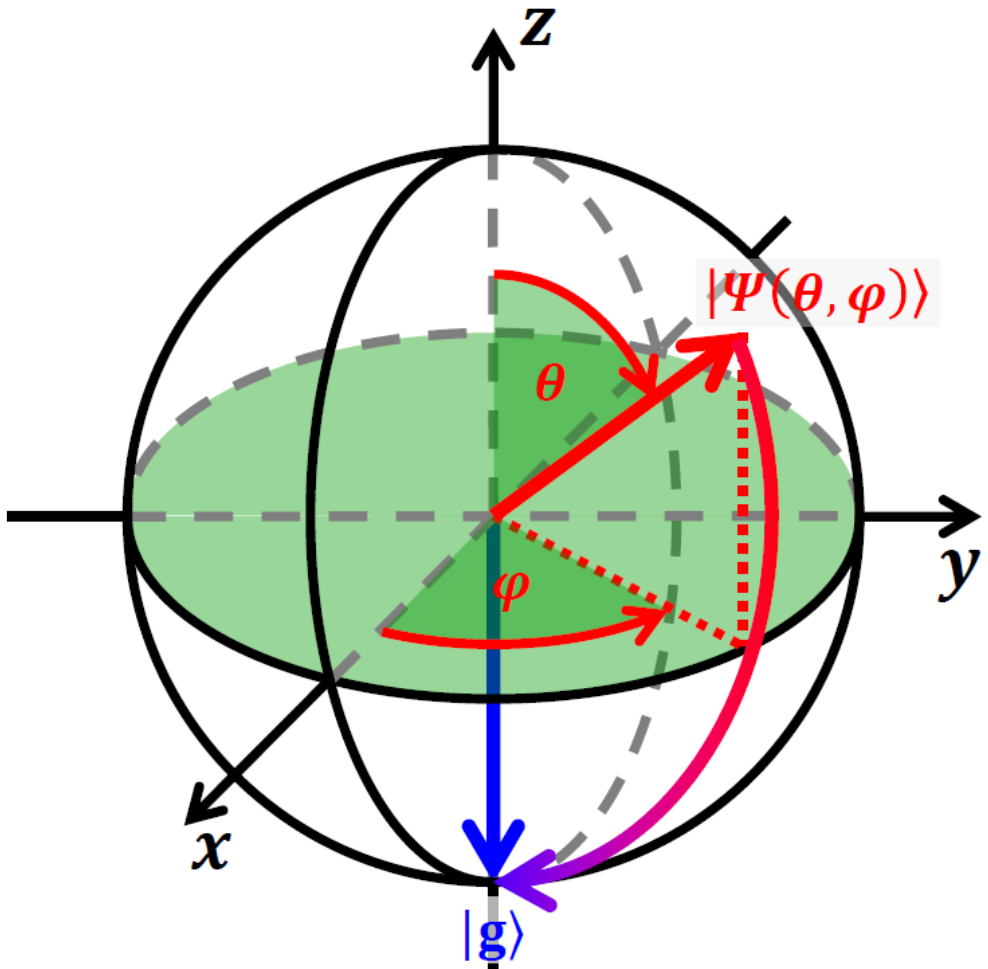
Dephasing in spectroscopic measurements



Dephasing in time-domain measurements



Energy Relaxation on the Bloch Sphere



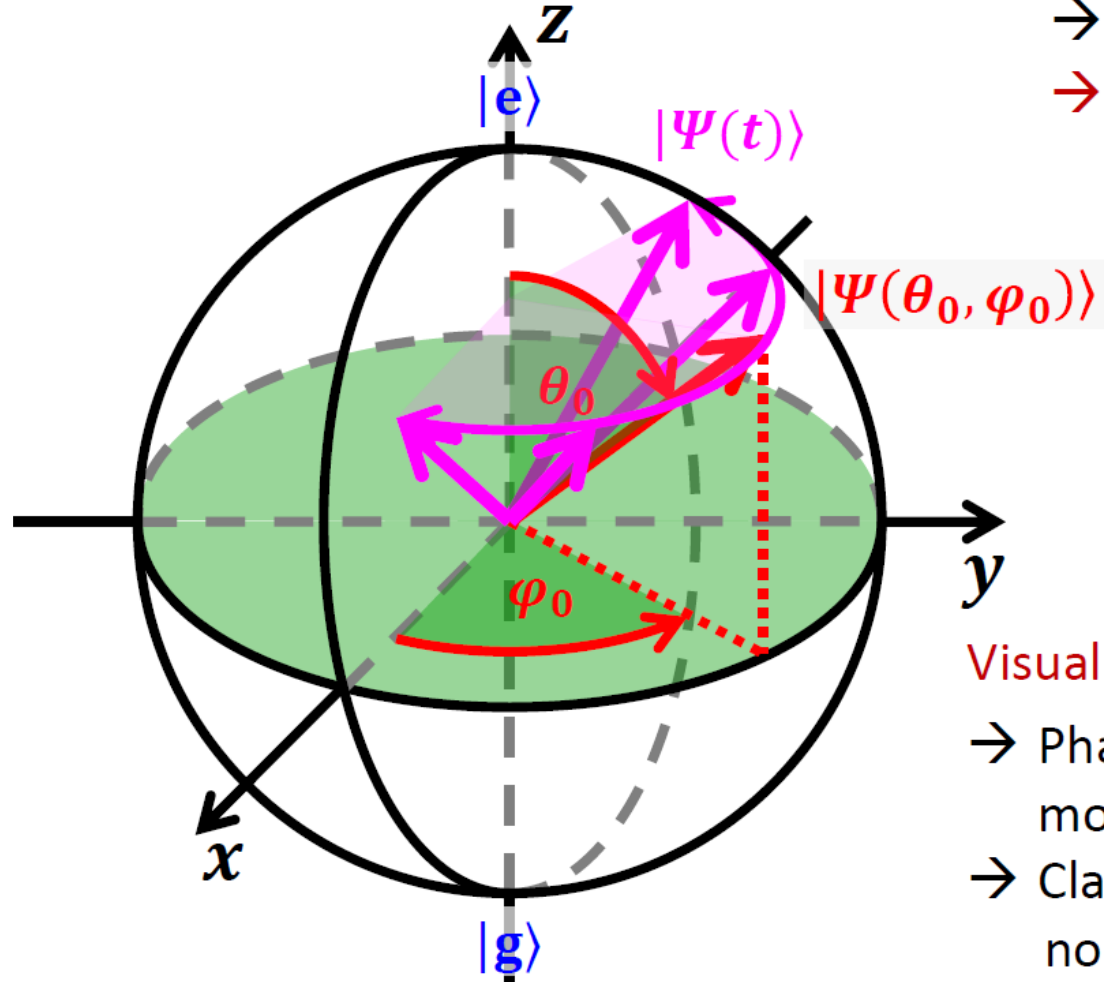
Environment induces energy loss

- State vector collapses to $|g\rangle$
- Implies also loss of phase information
- Intrinsically irreversible
- T_1 -time → rate $\Gamma_1 = \frac{2\pi}{T_1}$

Golden Rule argument

- $\Gamma_1 \propto S(\omega_q)$
- $S(\omega)$ is noise spectral density
- High frequency noise
- Intuition: Noise induces transitions

Dephasing on the Bloch Sphere



Environment induces random phase changes

- $\Gamma_\varphi \propto S(\omega \rightarrow 0)$, $T_\varphi = \frac{2\pi}{\Gamma_\varphi}$, (for Markovian bath)
- Low-frequency noise is detuned from ω_q
- No energy transfer

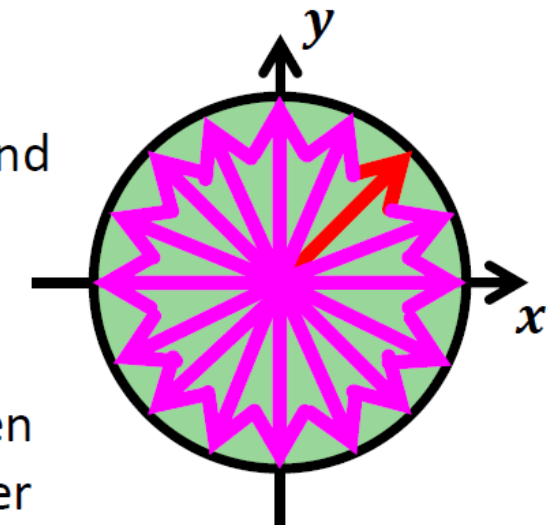
→ $1/f$ -noise → $S(\omega) \propto \frac{1}{\omega}$

- Example: two-level fluctuator bath
- To some extent reversible

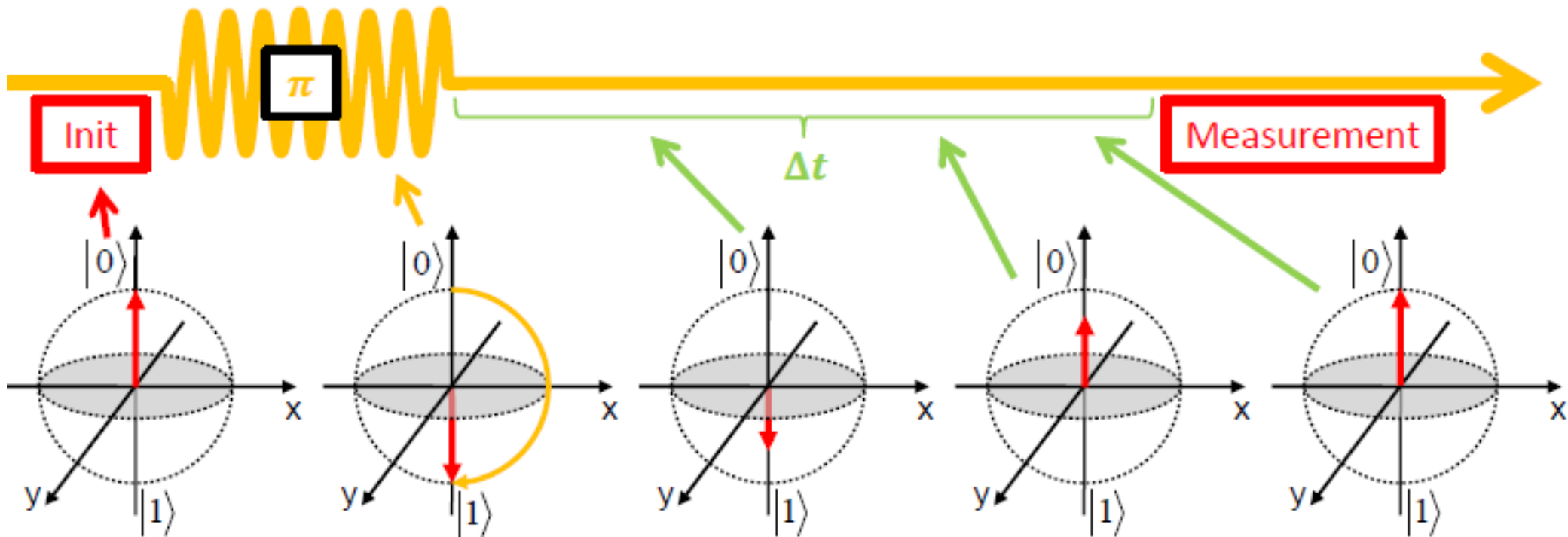
→ Decay laws $e^{-\frac{t}{T_\varphi}}$, $e^{-\left(\frac{t}{T_\varphi}\right)^2}$, $\left(\frac{t}{T_\varphi}\right)^\beta$

Visualization

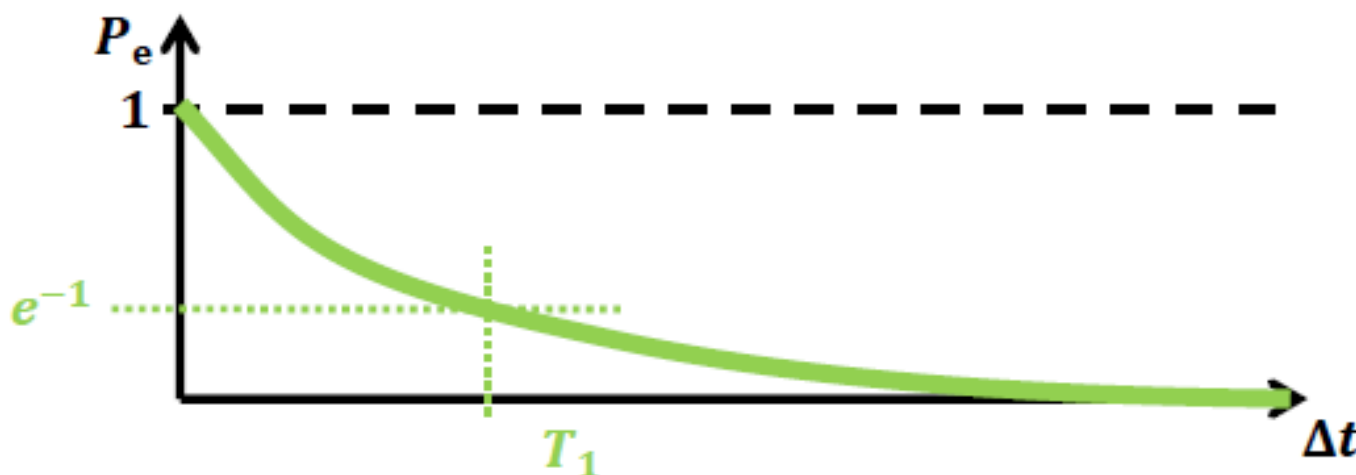
- Phase φ becomes more and more unknown with time
- Classical probability, no superposition!
- Phase coherence lost when arrows are distributed over whole equatorial plane



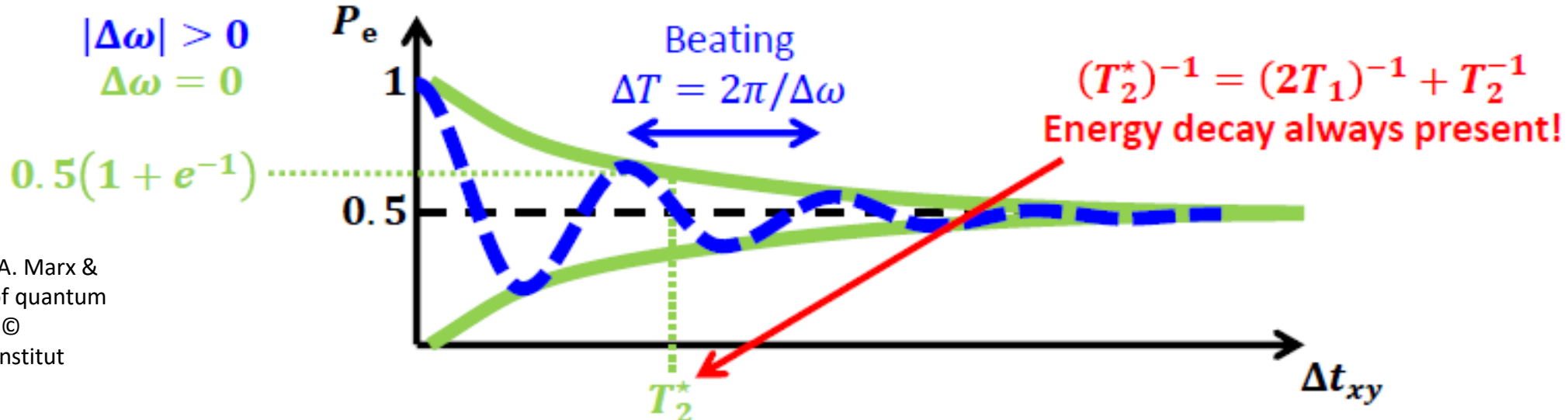
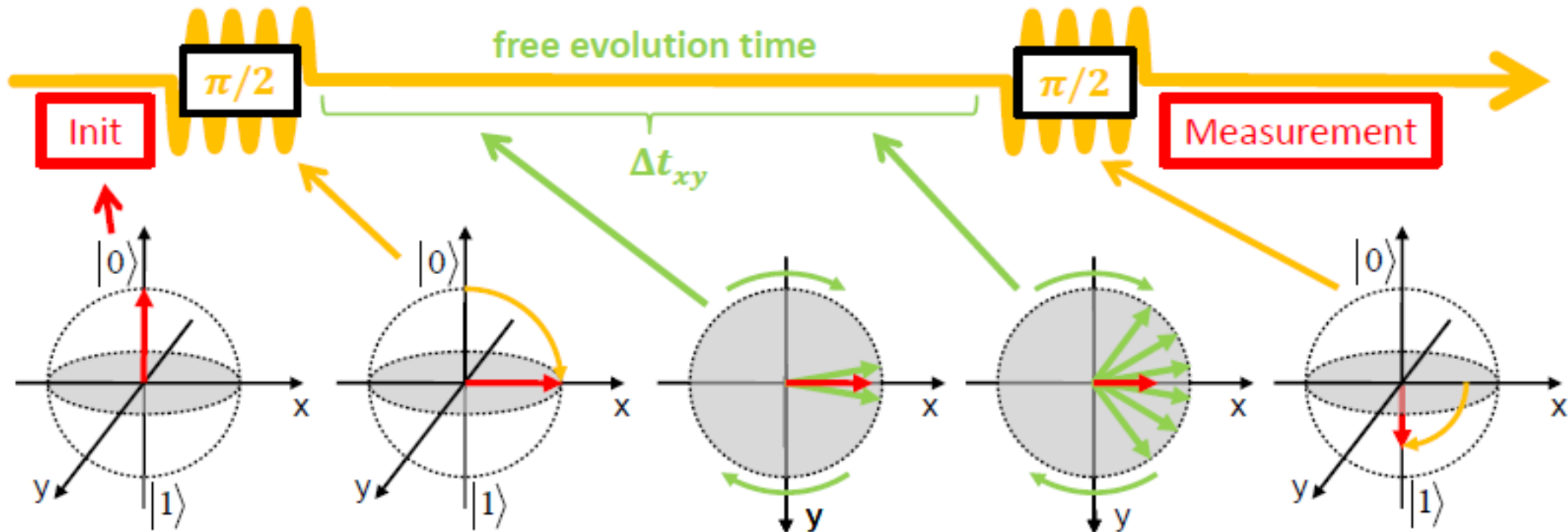
Qubit dynamics – Relaxation (T_1)



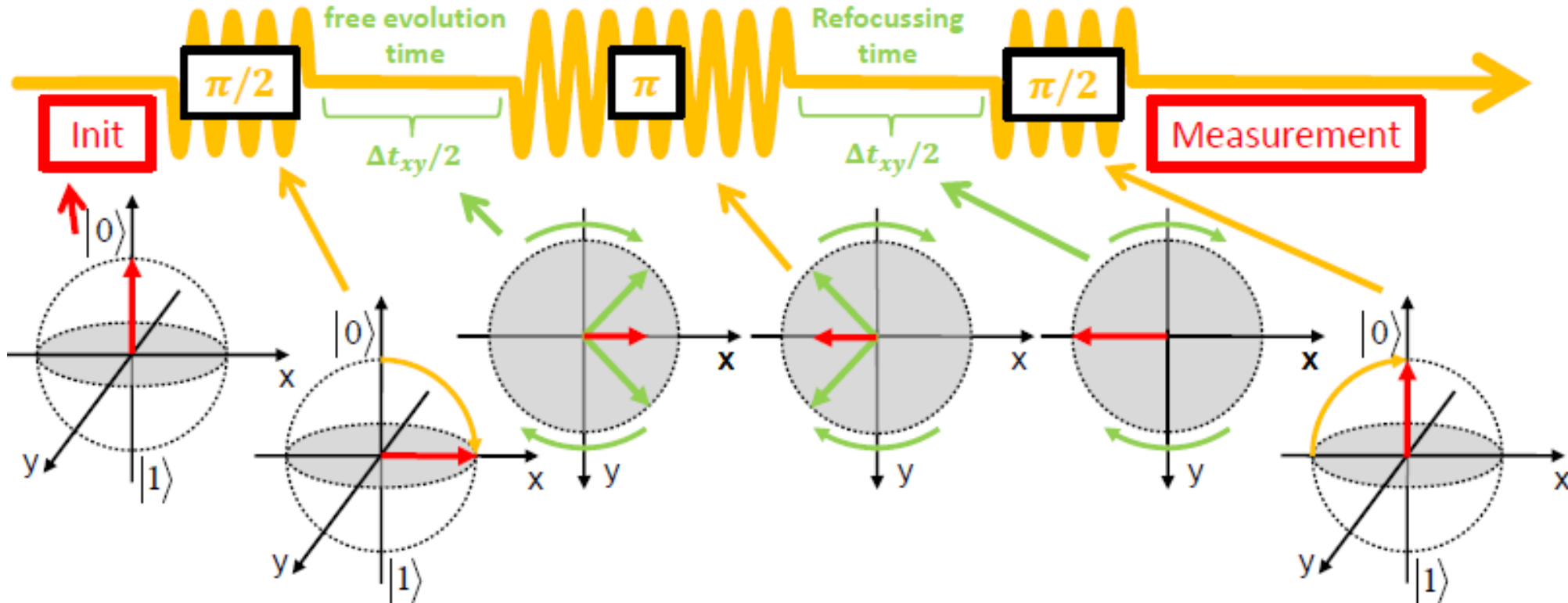
Rotating frame & no detuning ($\Delta\omega = \omega - \omega_q = 0$) \rightarrow no xy -evolution



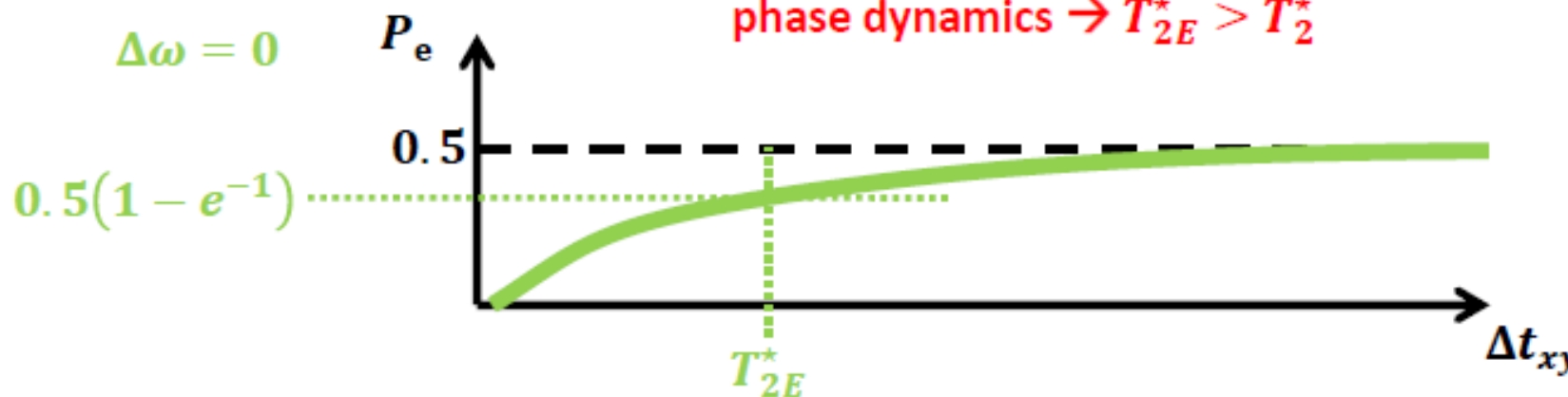
Qubit dynamics – Ramsey fringes (T_2^*)



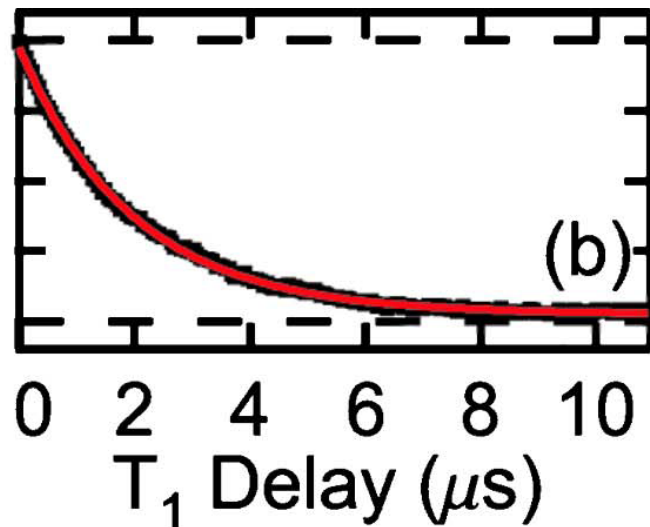
Qubit dynamics – Spin Echo (T^*_{2E})



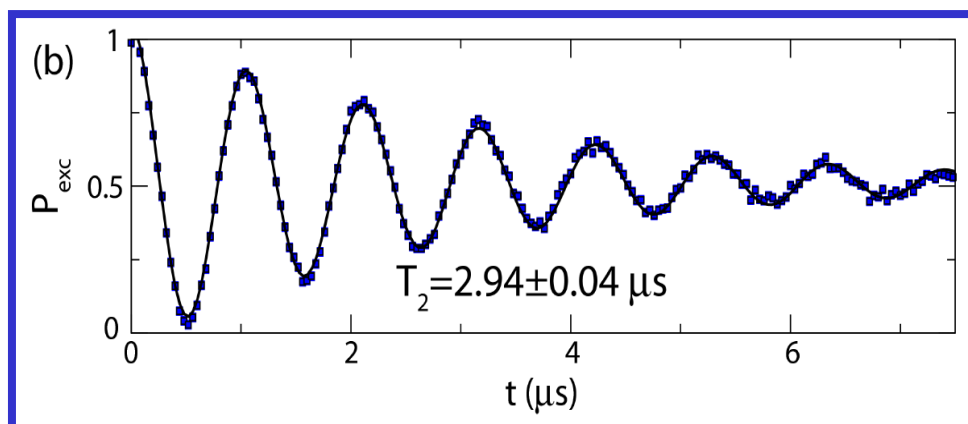
Refocussing pulse reverses low-frequency
phase dynamics $\rightarrow T^*_{2E} > T^*_2$



Coherence times of the first Transmon



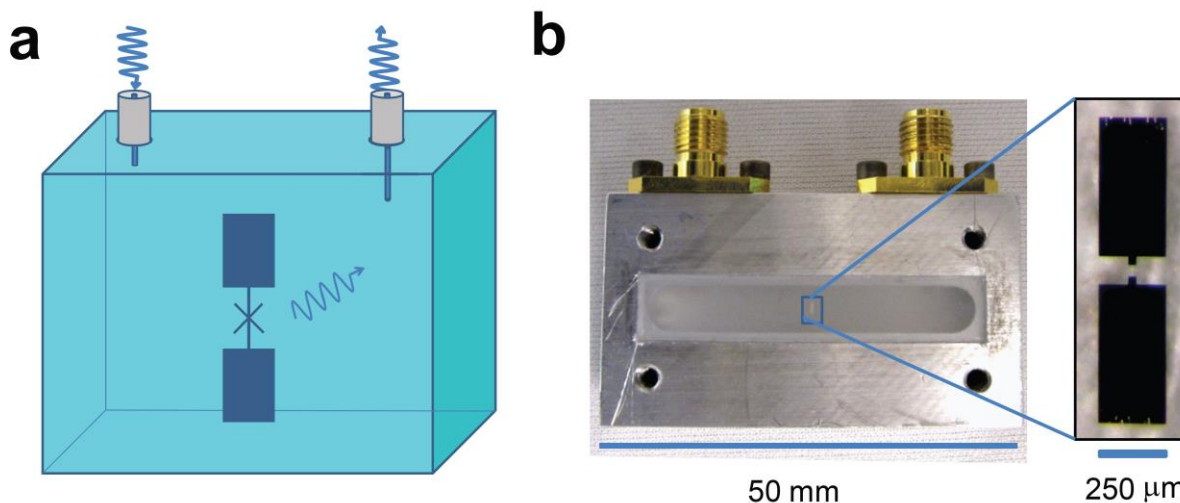
$$T_1 = 1-2 \mu\text{s}$$



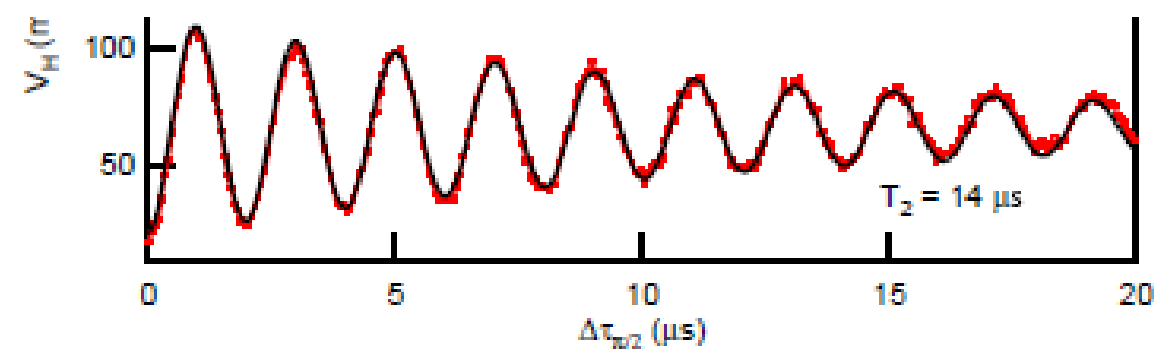
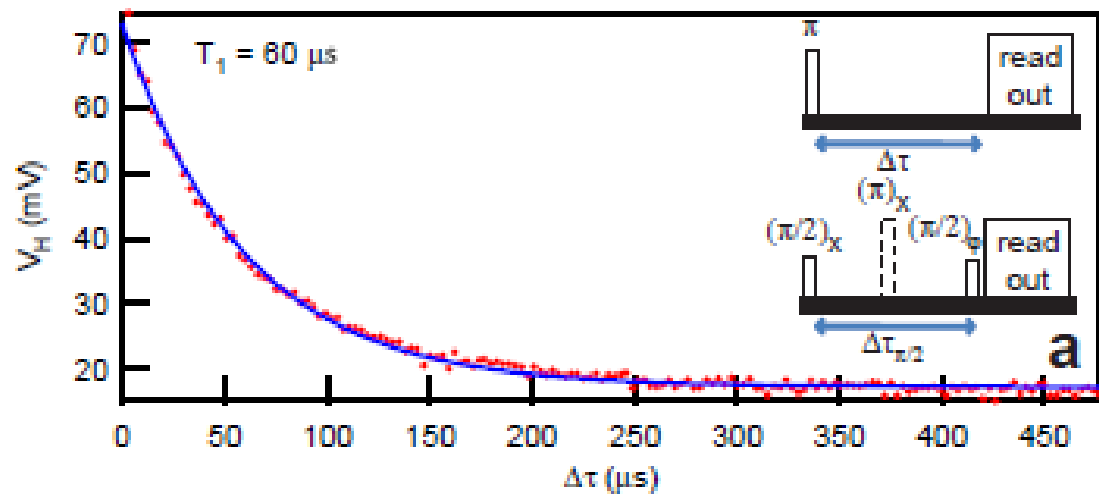
$$T_2 = 1-3 \mu\text{s}$$

Transmon in 3D cavity

H. Paik et al.,
Phys. Rev. Lett. **107**, 240501 (2011)

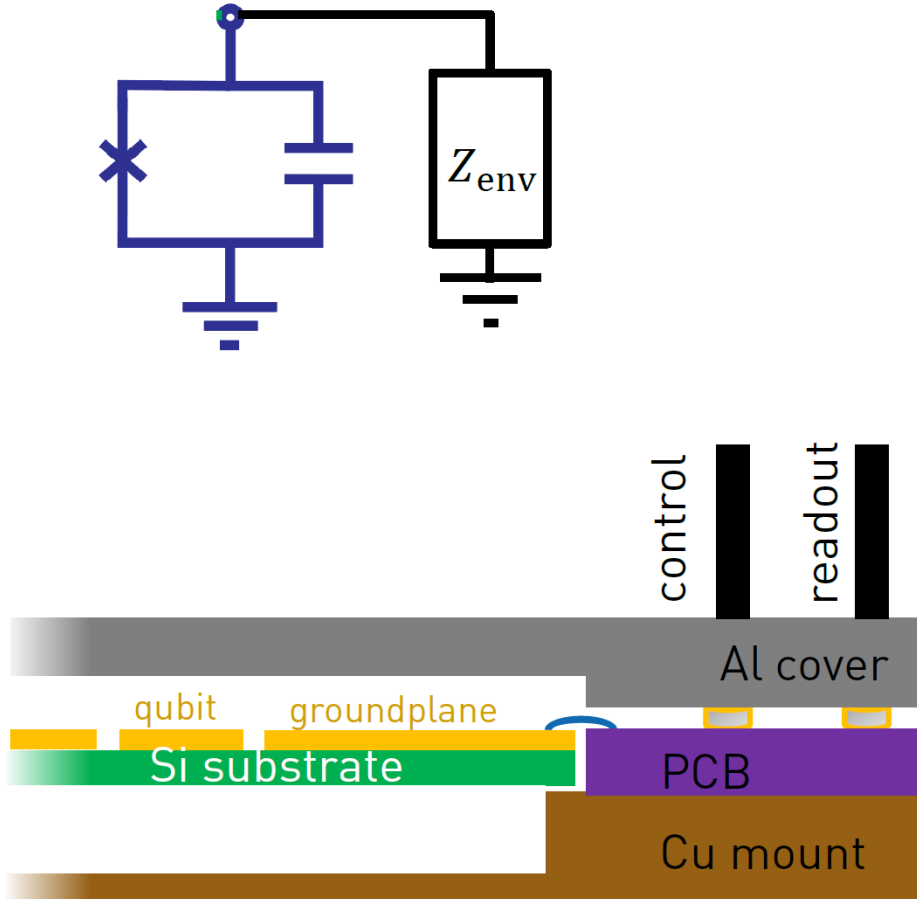


$$T_1 = 60 \mu\text{s}$$
$$T_2 = 15 \mu\text{s}$$



ULTIMATE LIMITS ON COHERENCE TIMES UNKNOWN YET

Relaxation due to the coupling to the electromagnetic environment



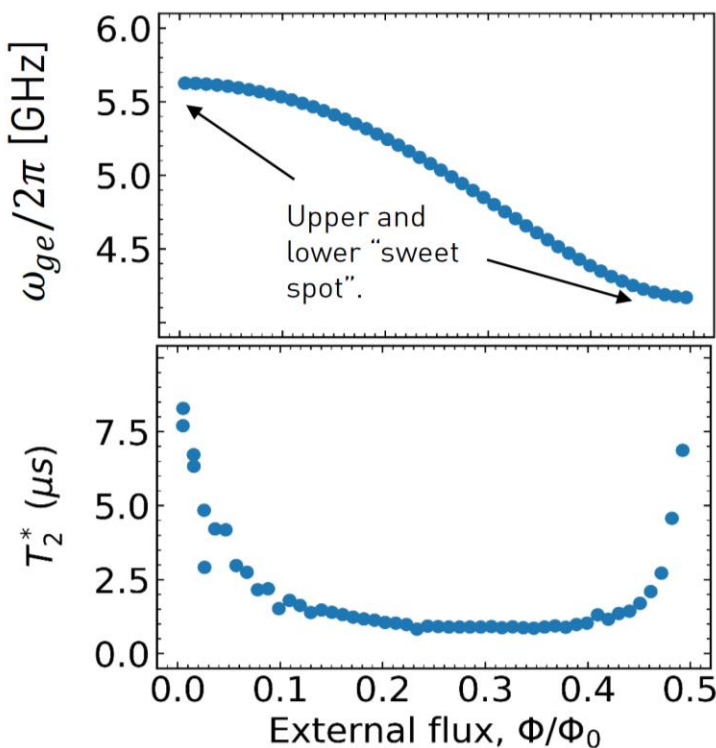
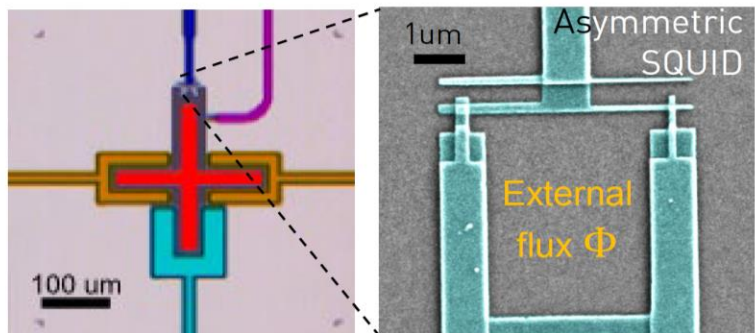
Mechanisms induced by control and readout:

- Purcell decay into readout lines. Mitigate by incorporating Purcell filters.
- Decay into charge control lines. Mitigate by designing coupling $\gamma \ll 1/T_1$. Compensate weaker coupling by stronger pulse.

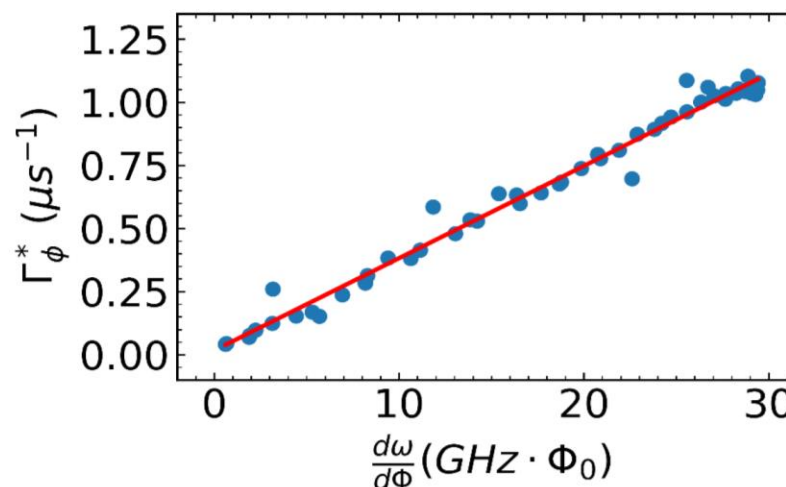
Packaging and housing

- Resistive loss imposed by stray capacitive coupling to non-SC elements such as Cu. Avoid by designing the qubits to have well-localized mode volume; keep distance from the edge of the chip,
- Coupling to box modes of the sample enclosure, e.g. in the substrate below the qubits. Mitigate by introducing recess below chip to lift frequency of box modes. Required for larger chip size: Through Silicon Vias (TSVs) and backside metallization, and additional top chip connected via bump bonds.

Sources of Dephasing: Flux noise



- Experiment: Measure qubit frequency ω_{ge} and T_2^* vs. external flux Φ .
- T_2^* longest at the bias points with vanishing gradient $\frac{d\omega_{ge}}{d\Phi} = 0$ (first order insensitive to magnetic flux noise).
- Pure dephasing rate Γ_ϕ^* is proportional to $\frac{d\omega_{ge}}{d\Phi}$.
- Slope proportional to flux noise density A and SQUID loop area.
- Typical values found in experiments $A \sim 10^1 - 10^3 n\Phi_0/\mu\text{m}^2$.
- Ambient magnetic noise shielded using mu-metal and superconducting cylinders around sample.
- LP and HP filters on flux control lines to suppress noise on flux control line.



$$\frac{\Gamma_\phi^*}{2\pi} = \frac{1}{T_\phi^*} = \frac{1}{T_2^*} - \frac{1}{2T_1}$$

Compare Hutchings et al.,
PRApplied, 8, 044003 (2017)

from C. Eichler (ETH)

Quasiparticle-induced qubit relaxation

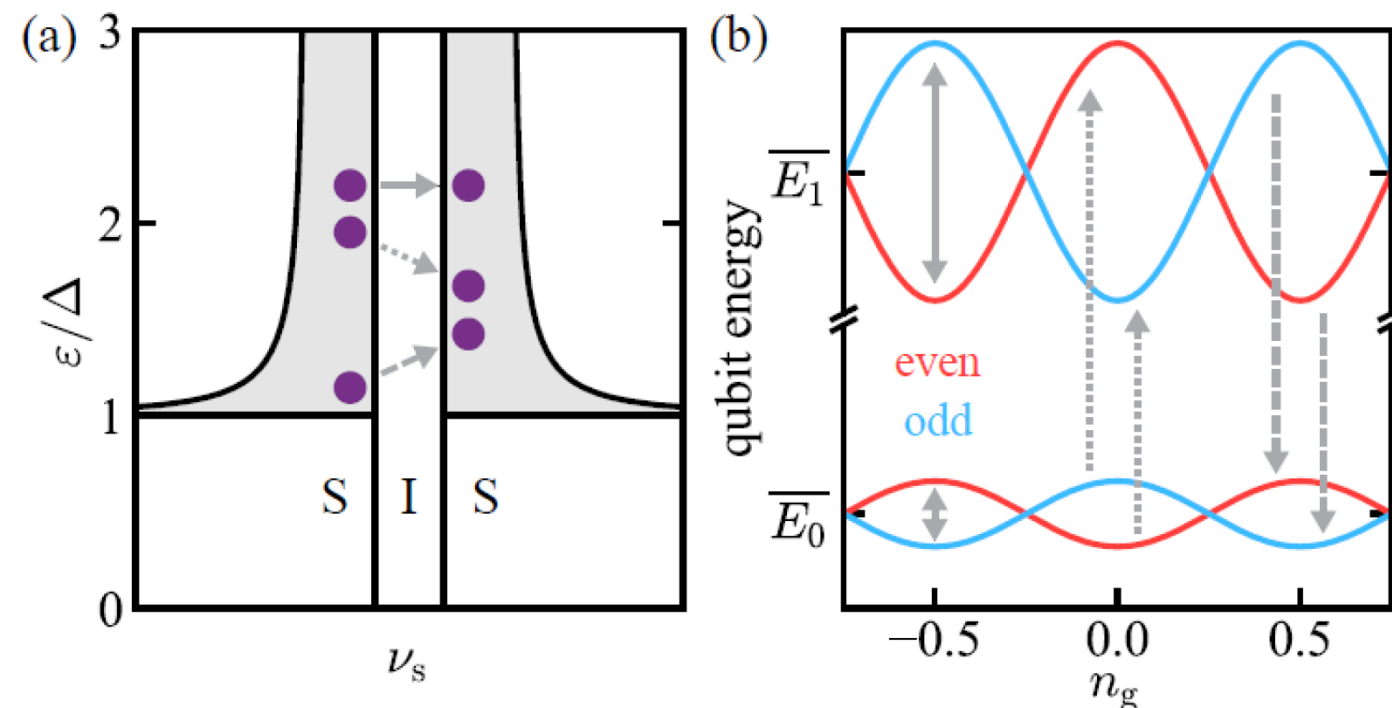


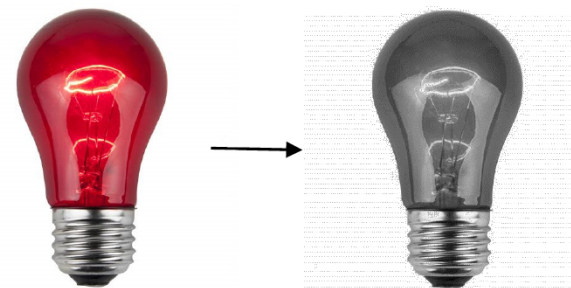
Figure from Serniak et al., PRL 121, 157701 (2018)

Further reading:

Catelani et al., PRB, (2011)

Riste et al., Nat. Comm. (2013)

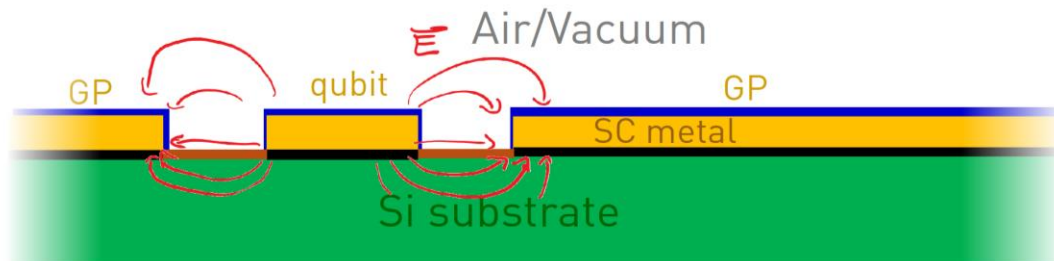
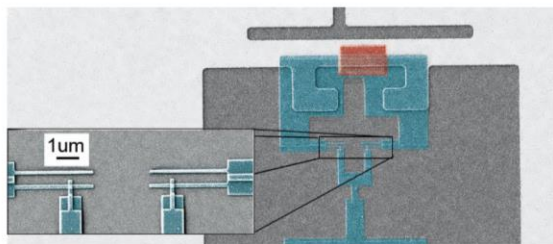
Hosseinkhani et al., PR Applied (2017)



- Aluminum superconducting gap energy $2\Delta/h = 100$ GHz.
- Tunneling of quasi particles changes parity of the offset charge and can induce qubit states transitions.
- At typical cryogenic temperature of ~ 20 mK in thermal equilibrium quasiparticles density should be exponentially suppressed.
- Experiments find higher quasiparticle density (relative to Cooper pair density) $x_{QP} \sim 10^{-8} - 10^{-6}$.
- Measured transition rates between states suggest that quasiparticles are not in thermal equilibrium.
- Mitigation: Avoid infrared (IR) radiation entering the sample box: light-tight sample enclosure, IR filter on control lines.

from C. Eichler (ETH)

Relaxation induced by two-level systems ensembles



Interfaces:

Metal-Substrate (MS), Substrate-Air (SA), Metal-Air (MA)

Selected references:

Review: C. Müller et al., Rep. Prog. Phys. (2019)

Lisenfeld et al., arXiv: 1909.09749

Wang et al., PRL 107, 162601 (2015)

- Superconducting Circuits are fabricated using multiple steps of thin film deposition, lithography, etching, lift-off. Depending on the details of processing, cleaning, and choice of materials: Material defects get introduced, which mostly reside at the interfaces.
- Common model: Defects described by effective two-level systems (TLS), which couple via dipole moment to the oscillating electric field of the qubit.
- Quality factor $Q = T_1 \omega_{ge}$ of the qubit given by

$$Q^{-1} = \sum_i p_i \tan\delta_i \quad \begin{matrix} \text{Sum over all materials} \\ \text{and interfaces} \end{matrix}$$

- Participation ratio $p_i = \frac{\int_{V_i} dV \epsilon_i |E|^2}{\int_{V_{tot}} dV \epsilon |E|^2}$, can be controlled by the design of the qubit capacitors.
- Loss tangent $\tan\delta_i$ material property proportional to the density of TLS.
- Intense research efforts aim at improving the understanding of underlying physical mechanisms and to develop better fabrication processes.

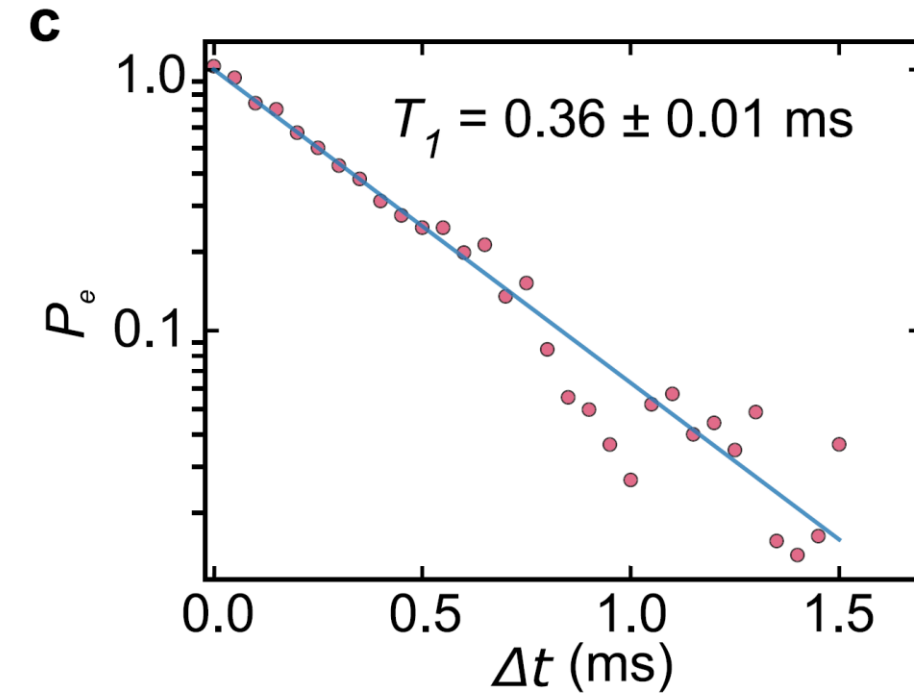
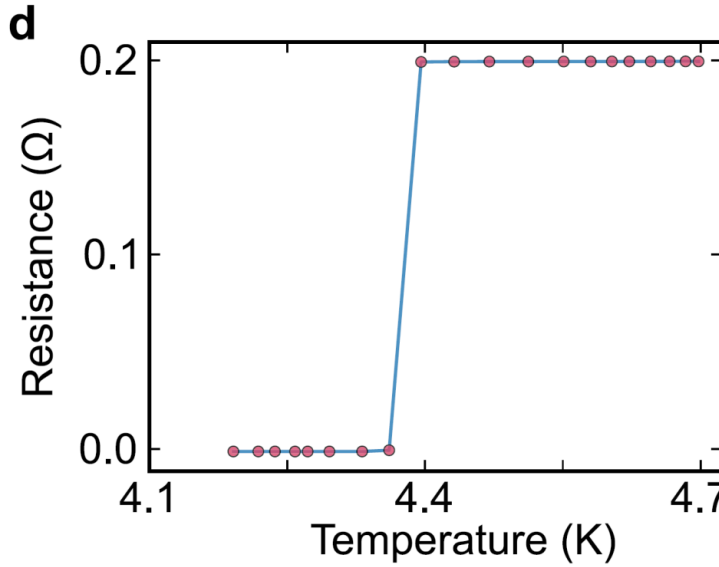
ARTICLE

<https://doi.org/10.1038/s41467-021-22030-5>

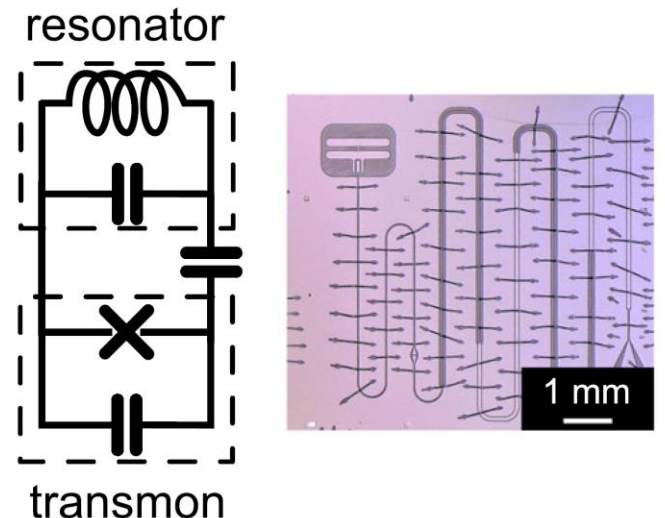
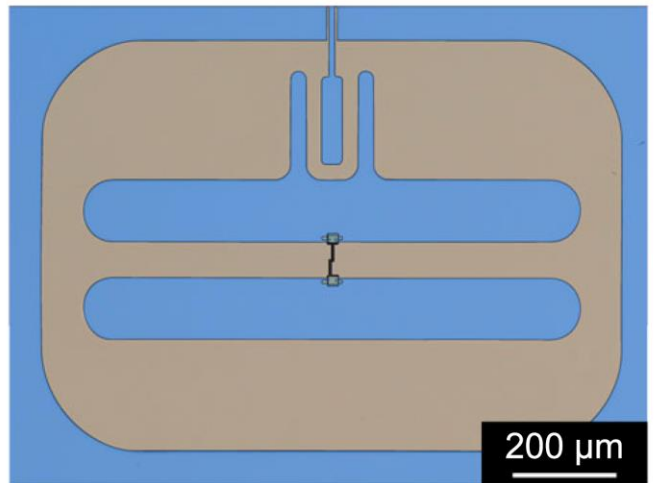
OPEN

 Check for updates

New material platform for superconducting transmon qubits with coherence times exceeding 0.3 milliseconds

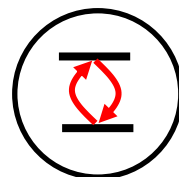


a

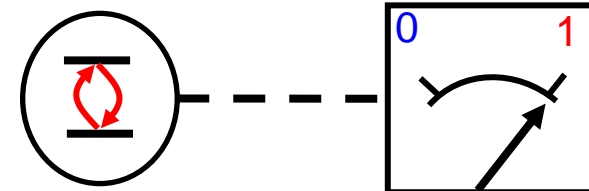


Requirements for QC

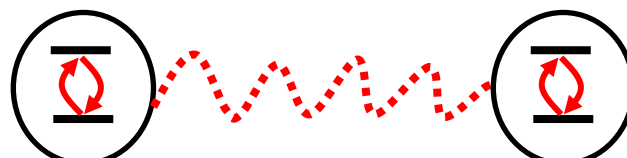
High-Fidelity Single Qubit Operations



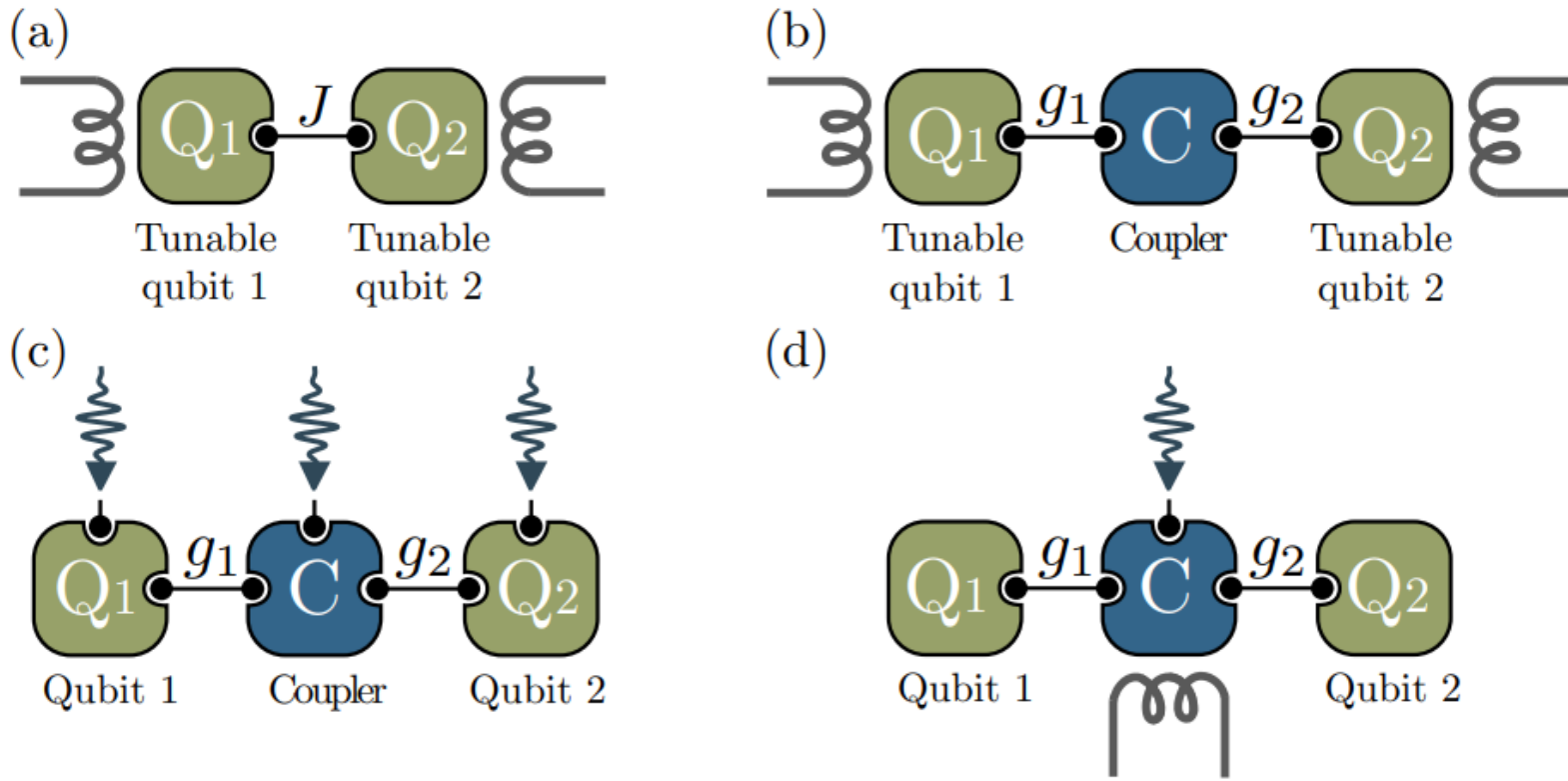
High-Fidelity Readout of Individual Qubits



Deterministic, On-Demand
Entanglement between Qubits



Two-qubits gate

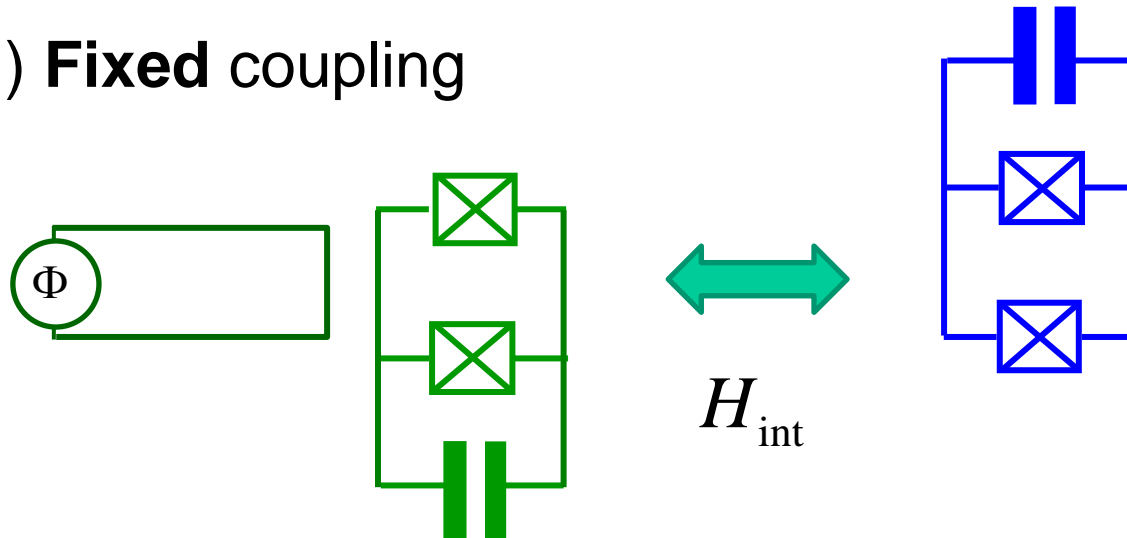


- Two-qubit gates are generally more challenging to realize than single-qubit gates. Error rates for current two-qubit gates are typically around one to a few percent, which is an order of magnitude higher than those of single-qubit gates.
- A key challenge in realizing two-qubit gates is the ability to rapidly turn interactions on and off. While for single-qubit gates this is done by simply turning on and off a microwave drive, two-qubit gates require turning on a coherent qubit-qubit interaction for a fixed time. Achieving large on/off ratios is far more challenging in this situation.

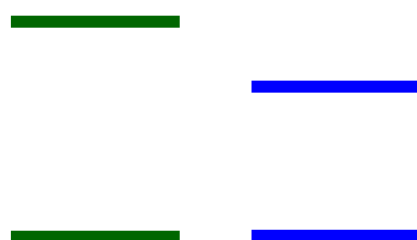
Schematic illustration of some of the two-qubit gate schemes. Exchange interaction between two qubits (a) from direct capacitive coupling or (b) mediated by a coupler such as a bus resonator. The qubits are tuned in and out of resonance with each other to activate and deactivate the interaction, respectively. (c) All-microwave gates activated by microwave drives on the qubits and/or a coupler such as a bus resonator. In this scheme, the qubits can have a fixed frequency. (d) Parametric gates involving modulating a system parameter, such as a tunable coupler.

Coupling strategies

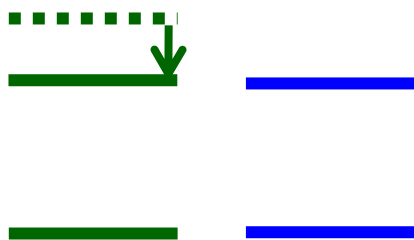
1) Fixed coupling



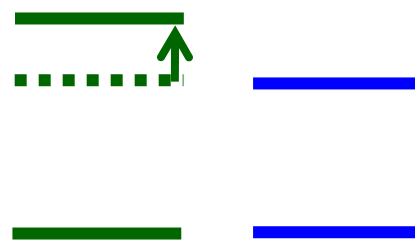
Entanglement on-demand ???
« Tune-and-go » strategy



Coupling
effectively OFF



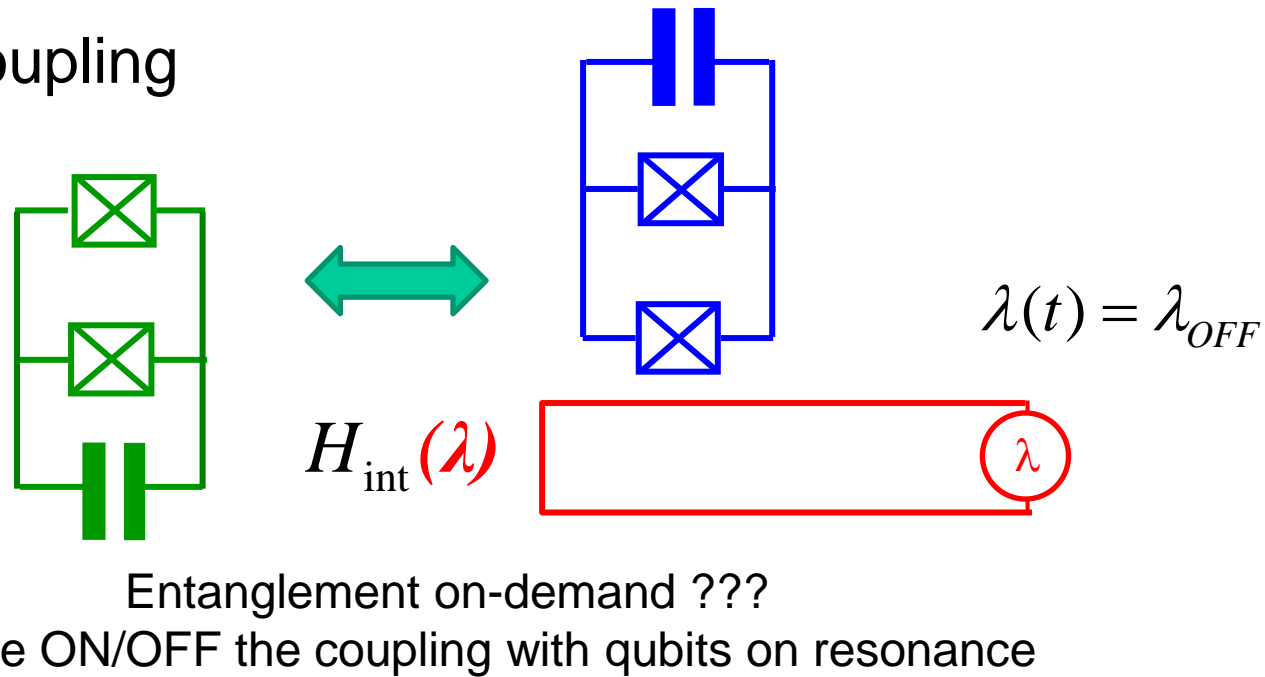
Coupling activated
in resonance for τ



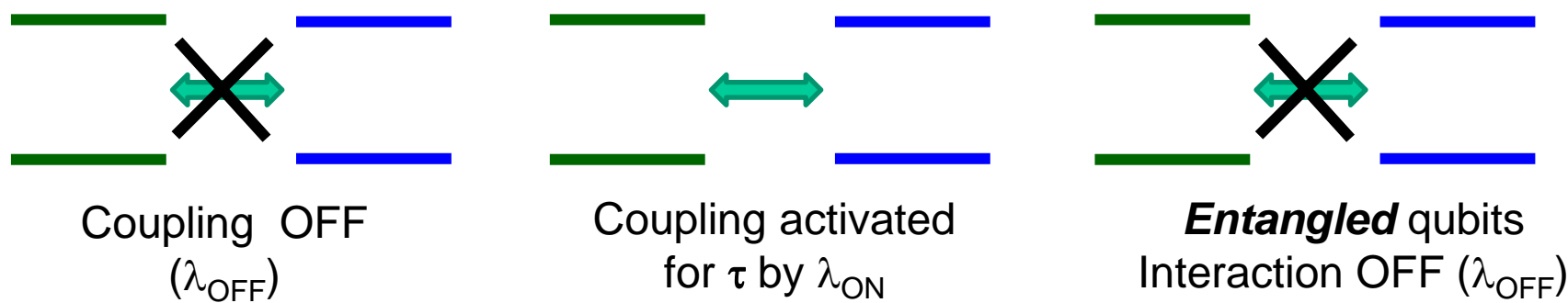
Entangled qubits
Interaction effectively OFF

Coupling strategies

2) Tunable coupling

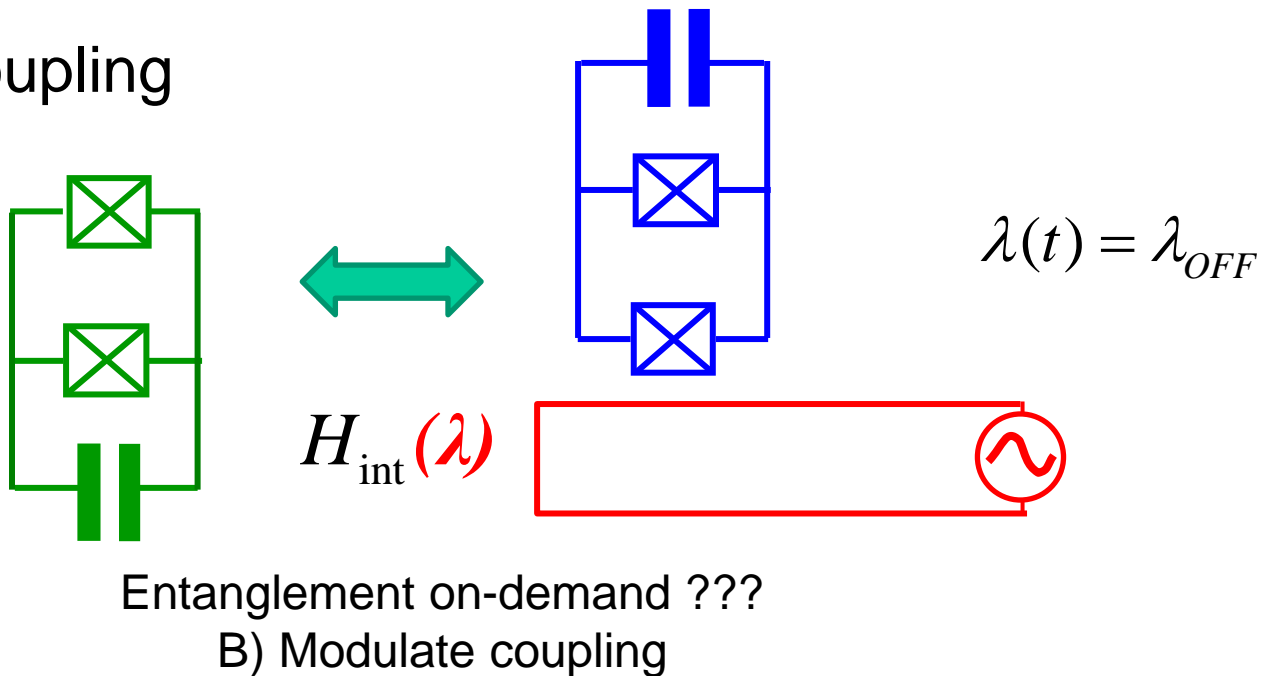


A) Tune ON/OFF the coupling with qubits on resonance

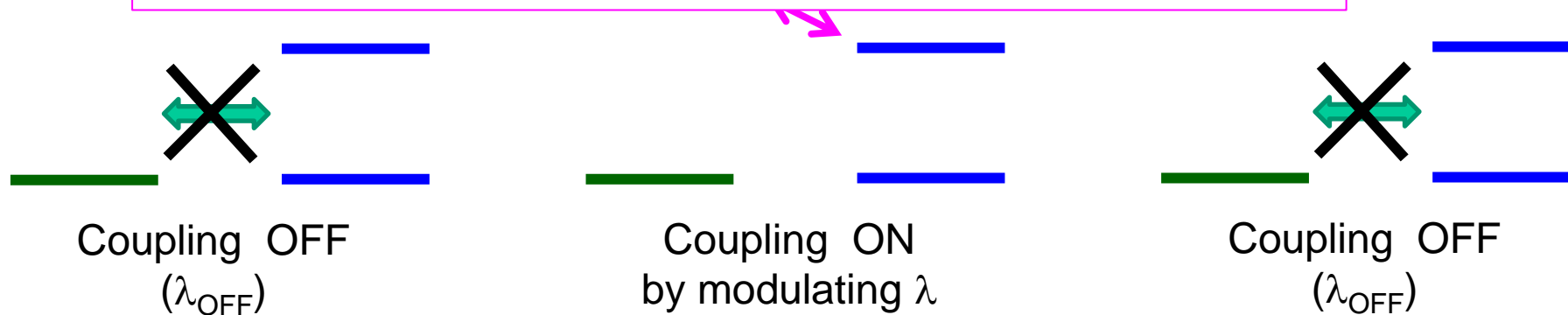


Coupling strategies

2) Tunable coupling

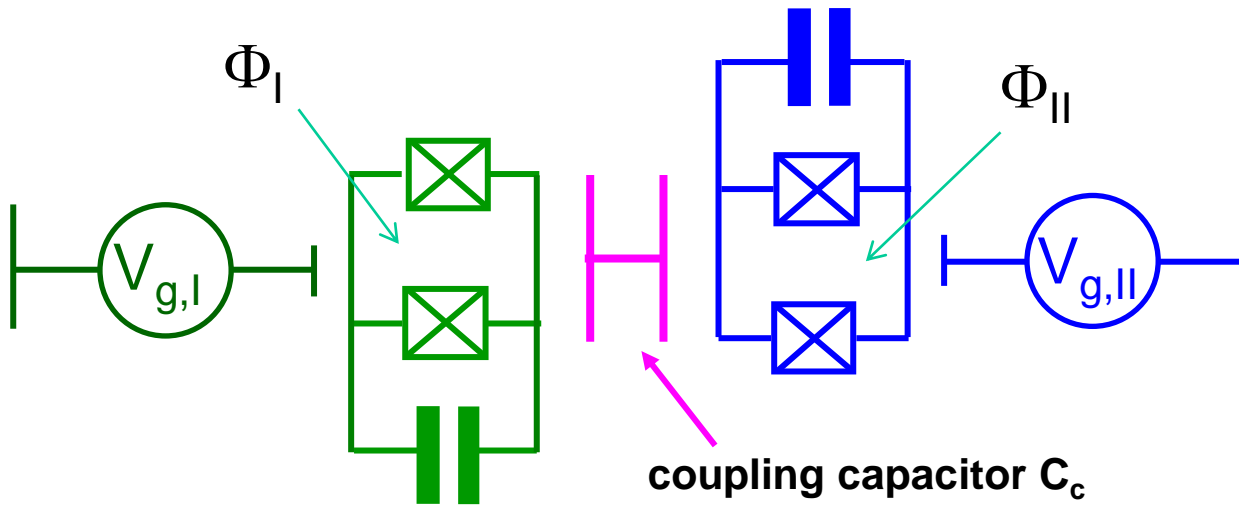


IN THIS LECTURE : ONLY FIXED COUPLING



Coupling strategies

1) Direct capacitive coupling



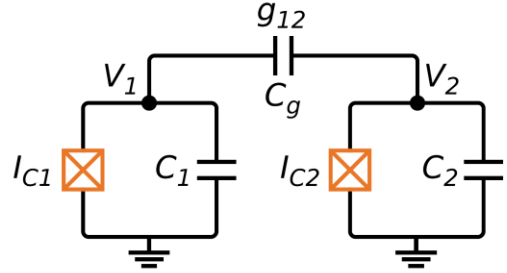
$$\begin{aligned}
 H = & E_{c,I}(\hat{N}_I - N_{g,I}) - E_{J,I}(\Phi_I) \cos \hat{\theta}_I \\
 + & E_{c,II}(\hat{N}_{II} - N_{g,II}) - E_{J,II}(\Phi_{II}) \cos \hat{\theta}_{II} \\
 + & 2 \frac{E_{c,I} E_{c,II}}{E_{cc}} (\hat{N}_I - N_{g,I})(\hat{N}_{II} - N_{g,II})
 \end{aligned}$$

$$\hbar g = (2e)^2 \frac{C_c}{C_I C_{II}} \left| \langle 0_I | \hat{N}_I | 1_I \rangle \langle 0_{II} | \hat{N}_{II} | 1_{II} \rangle \right|$$

$$\begin{cases}
 H_{q,I} = -\frac{\hbar \omega_{01}^I(\Phi_I)}{2} \sigma_{z,I} \\
 H_{q,II} = -\frac{\hbar \omega_{01}^{II}(\Phi_{II})}{2} \sigma_{z,II} \\
 H_c = \hbar g \sigma_{x,I} \sigma_{x,II} \\
 \sim \hbar g (\sigma_I^+ \sigma_{II}^- + \sigma_I^- \sigma_{II}^+)
 \end{cases}$$

courtesy CEA Saclay

(a) Direct capacitive coupling



Coupling strategies

1) Direct capacitive coupling

$$V \propto n \propto i(a - a^\dagger)$$

$$H = \sum_{i \in 1,2} \left[\omega_i a_i^\dagger a_i + \frac{\alpha_i}{2} a_i^\dagger a_i^\dagger a_i a_i \right] - g(a_1 - a_1^\dagger)(a_2 - a_2^\dagger)$$

$$H = H_1 + H_2 + H_{\text{int}}$$

$$H_{\text{int}} = C_g V_1 V_2$$

$$C_g \ll C_1, C_2$$

$$H = \sum_{i=1,2} [4E_{C,i}n_i^2 - E_{J,i} \cos(\phi_i)] + 4e^2 \frac{C_g}{C_1 C_2} n_1 n_2$$

where the expression within brackets represent the Duffing oscillator Hamiltonian for the qubits and g is the coupling energy. Since we define $V \propto n \propto i(a - a^\dagger)$, and consequently $I \propto \phi \propto (a + a^\dagger)$, the original $n_1 n_2$ -term becomes what is shown in Eq. (30). Such a coupling is called “transverse,” because the coupling Hamiltonian has nonzero matrix elements only at off-diagonal positions with respect to both oscillators, i.e., ${}_i\langle k | a_i - a_i^\dagger | k \rangle_i = 0$ for any integer k and for $i \in 1, 2$, and in this case, ${}_i\langle k \pm 1 | a_i - a_i^\dagger | k \rangle_i \neq 0$.

If we can ignore higher energy levels ($k \geq 2$) either because of sufficient anharmonicity or through careful control protocols that ensure these levels never have influence, we may truncate the Hamiltonian in Eq. (30) to

$$H = \sum_{i \in 1,2} \frac{1}{2} \omega_i \sigma_{z,i} + g \sigma_{y,1} \sigma_{y,2} \quad (31)$$

$$H_{qq} = g\sigma_{y1} \otimes \sigma_{y2}$$

$$g \rightarrow g_{q-q} = \frac{1}{2} \sqrt{\omega_{q1}\omega_{q2}} \frac{C_{q-q}}{\sqrt{C_{q-q} + C_1}\sqrt{C_{q-q} + C_2}}, \quad (104)$$

where C_{q-q} is the qubit-qubit coupling capacitance and C_i is the capacitance of qubit i . Throughout this section, we will assume a direct capacitive coupling between qubits of the flux-tunable transmon type, so that $g = g_{q-q}$ and $\omega_{qi} \rightarrow \omega_{qi}(\Phi_i)$. For simplicity, we suppress the explicit flux dependence of the ω_{qi} 's and simply refer to the coupling as g . Equation (102) can be rewritten as

$$H_{qq} = -g([\sigma^+ - \sigma^-] \otimes [\sigma^+ - \sigma^-]), \quad (105)$$

and then using the rotating wave approximation again (i.e., dropping fast rotating terms) we arrive at

$$H_{qq} = g(e^{i\delta\omega_{12}t}\sigma^+\sigma^- + e^{-i\delta\omega_{12}t}\sigma^-\sigma^+), \quad (106)$$

where we have introduced the notation $\delta\omega_{12} = \omega_{q1} - \omega_{q2}$ and suppressed the explicit tensor product between qubit subspaces. If we now change the flux of qubit 1 to bring it into resonance with qubit 2 ($\omega_{q1} = \omega_{q2}$), then

$$H_{qq} = g(\sigma^+\sigma^- + \sigma^-\sigma^+) = \frac{g}{2}(\sigma_x\sigma_x + \sigma_y\sigma_y). \quad (107)$$

The first part of Eq. (107) shows that a capacitive interaction leads to a swapping of excitations between the two qubits, giving rise to the “swap” in *iSWAP*. Moreover, due to the last part of Eq. (107), this capacitive coupling is also sometimes said to give rise to an “XY” interaction.²¹¹ The unitary corresponding to a XY (swap) interaction is

$$U_{qq}(t) = e^{-\frac{i\pi}{2}(\sigma_x\sigma_x + \sigma_y\sigma_y)t} = \begin{bmatrix} 1 & 0 & 0 & 0 \\ 0 & \cos(gt) & -i\sin(gt) & 0 \\ 0 & -i\sin(gt) & \cos(gt) & 0 \\ 0 & 0 & 0 & 1 \end{bmatrix}. \quad (108)$$

Since the qubits are tunable in frequency, we can now consider the effect of tuning the qubits into resonance for a time $t' = \frac{\pi}{2g}$

$$U_{qq}\left(\frac{\pi}{2g}\right) = \begin{bmatrix} 1 & 0 & 0 & 0 \\ 0 & 0 & -i & 0 \\ 0 & -i & 0 & 0 \\ 0 & 0 & 0 & 1 \end{bmatrix} \equiv i\text{SWAP}. \quad (109)$$

From this result, we see that a capacitive coupling between qubits turned on for a time t' (inversely related to the coupling strength in units of radial frequency) leads to implementing a so called “*iSWAP*” gate,^{209,210,212–215} which acts to swap an excitation between the two qubits, and add a phase of $i = e^{i\pi/2}$. For completeness, we note that for $t'' = \frac{\pi}{4g}$, the resulting unitary

$$U_{qq}\left(\frac{\pi}{4g}\right) = \begin{bmatrix} 1 & 0 & 0 & 0 \\ 0 & 1/\sqrt{2} & -i/\sqrt{2} & 0 \\ 0 & -i/\sqrt{2} & 1/\sqrt{2} & 0 \\ 0 & 0 & 0 & 1 \end{bmatrix} \equiv \sqrt{i\text{SWAP}} \quad (110)$$

is typically referred to as the “squareroot-*iSWAP*” gate. The $\sqrt{i\text{SWAP}}$ gate can be used to generate Bell-like superposition states, e.g., $|01\rangle + i|10\rangle$.

iSWAP Gate

$$H / \hbar = -\frac{\omega_{01}^I}{2} \sigma_z^I - \frac{\omega_{01}^{II}}{2} \sigma_z^{II} + g (\sigma_+^I \sigma_-^{II} + \sigma_-^I \sigma_+^{II})$$

H_{int}

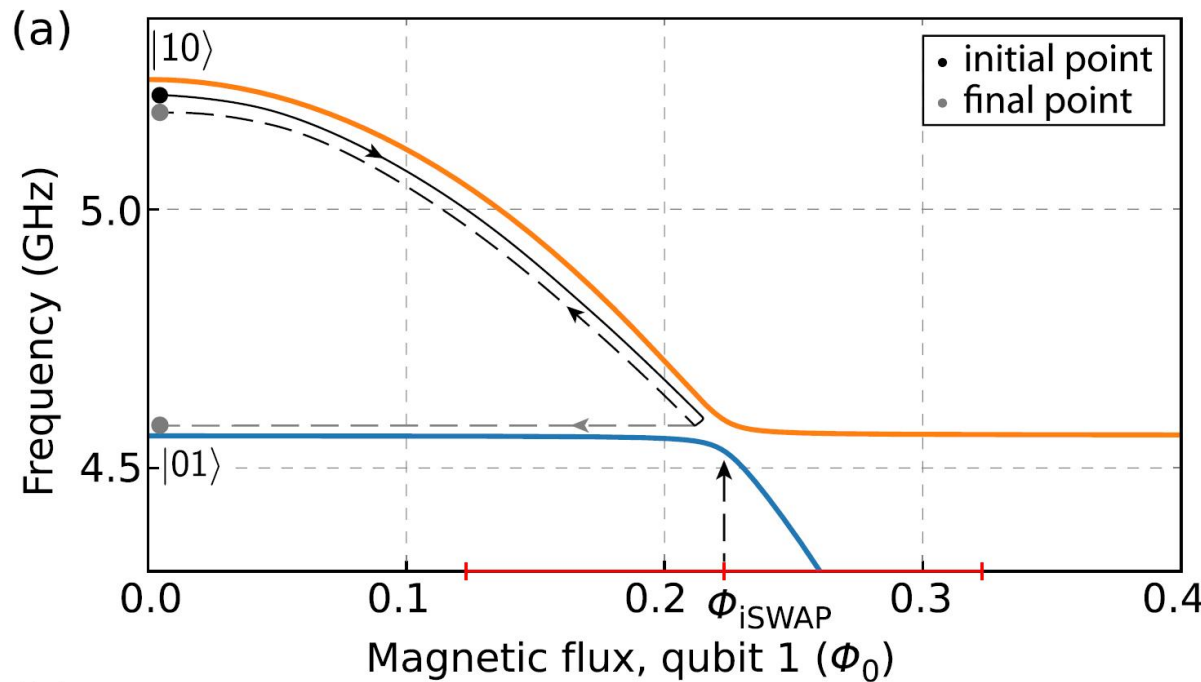
→ « Natural » universal gate : $\sqrt{i\text{SWAP}}$

On resonance, ($\omega_{01}^I = \omega_{01}^{II}$)

$$U_{\text{int}}(t) = \begin{bmatrix} \textbf{OO} & \textbf{1O} & \textbf{O1} & \textbf{11} \\ 1 & 0 & 0 & 0 \\ 0 & \cos(gt) & -i \sin(gt) & 0 \\ 0 & -i \sin(gt) & \cos(gt) & 0 \\ 0 & 0 & 0 & 1 \end{bmatrix} U_{\text{int}}\left(\frac{\pi}{2g}\right) = \boxed{\begin{bmatrix} 1 & 0 & 0 & 0 \\ 0 & 1/\sqrt{2} & -i/\sqrt{2} & 0 \\ 0 & -i/\sqrt{2} & 1/\sqrt{2} & 0 \\ 0 & 0 & 0 & 1 \end{bmatrix}} = \sqrt{i\text{SWAP}}$$

Coupling strategies: direct capacitive coupling

Experiment



Applied Physics Reviews 6, 021318 (2019)

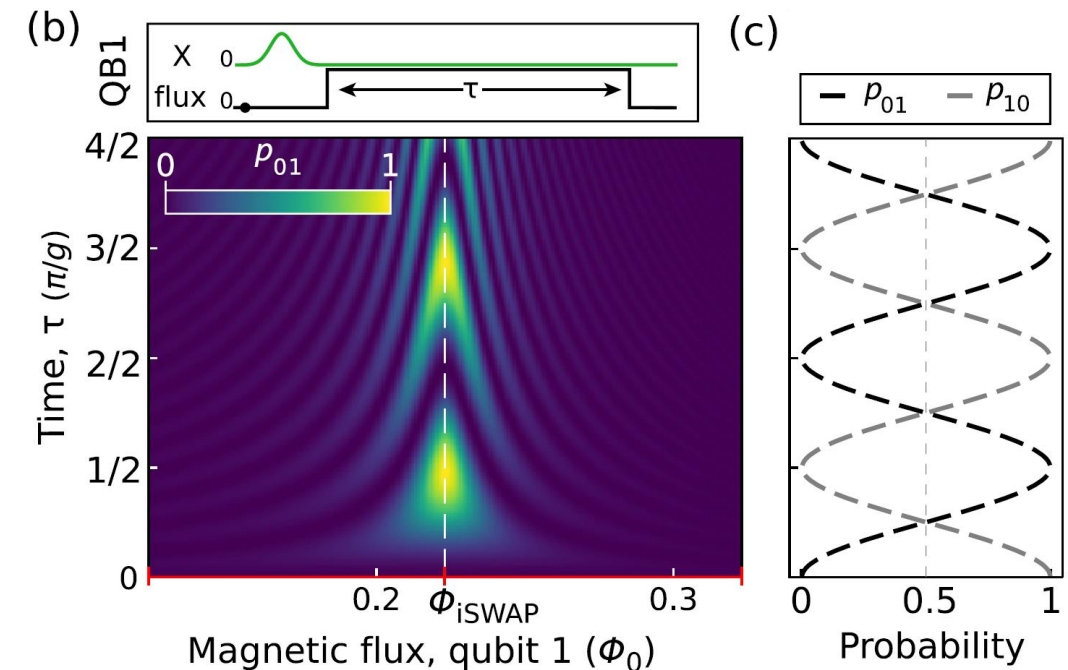
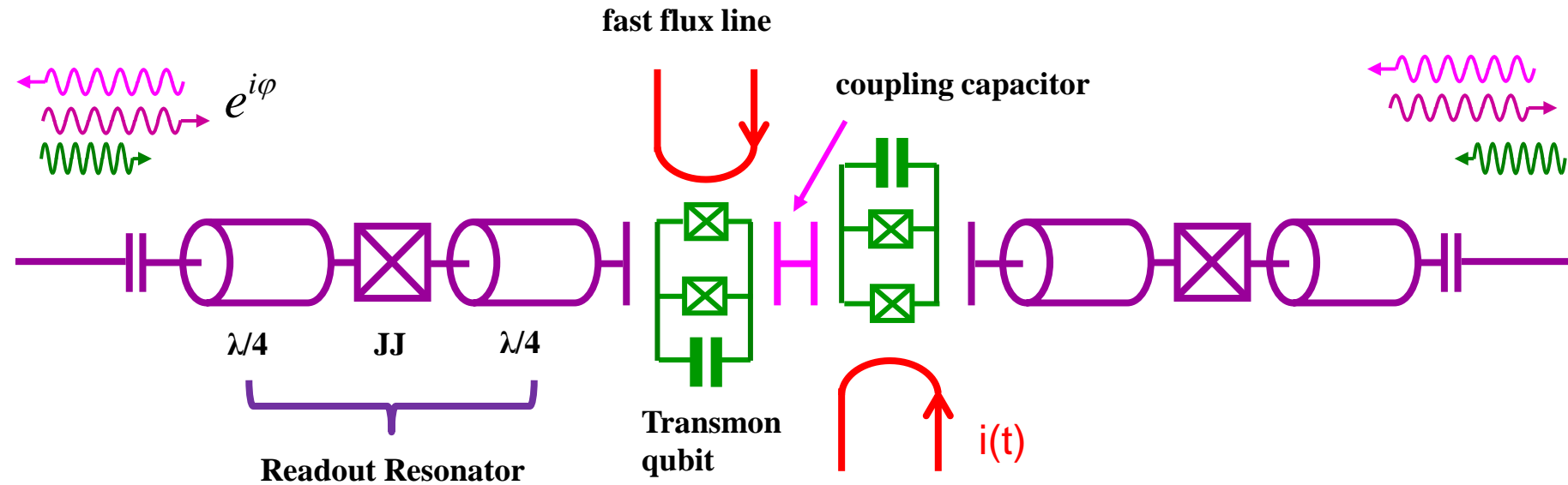
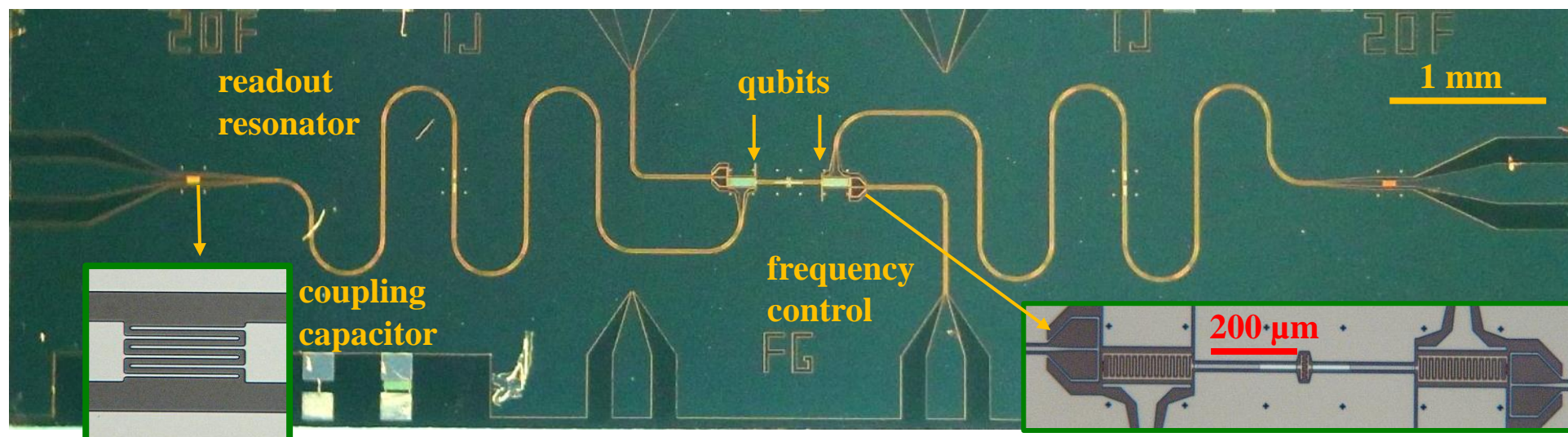


FIG. 15. (a) Spectrum of two transmon qubits (written in the combined basis as $|QB1, QB2\rangle$) as the local flux through the loop of qubit 1 is increased. The black/dashed lines with arrows indicate a typical flux trajectory to demonstrate operation of *iSWAP* gate. (b) Probability of swapping into the $|01\rangle$ state as a function of time and flux. The pulse sequence corresponds to preparing $|10\rangle$ and performing a typical *iSWAP* operation (for a time τ). (c) Probabilities of $|01\rangle$ (black) and $|10\rangle$ (gray) at $\Phi = \Phi_{iSWAP}$ [white dashed line in (b)] as the time spent at the operating point (τ) is increased. This simulation does not include any decay effects.

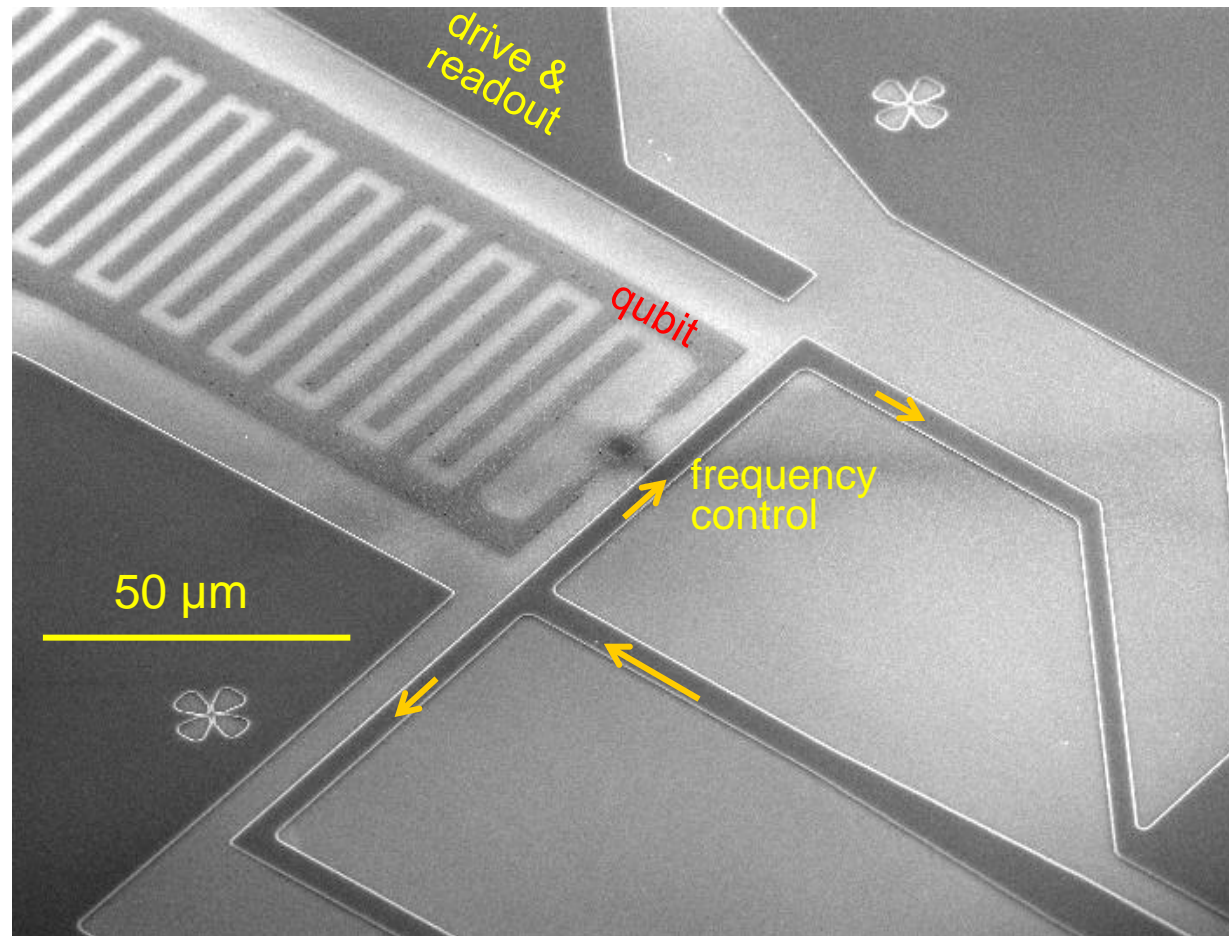
Example : capacitively coupled transmons with individual readout



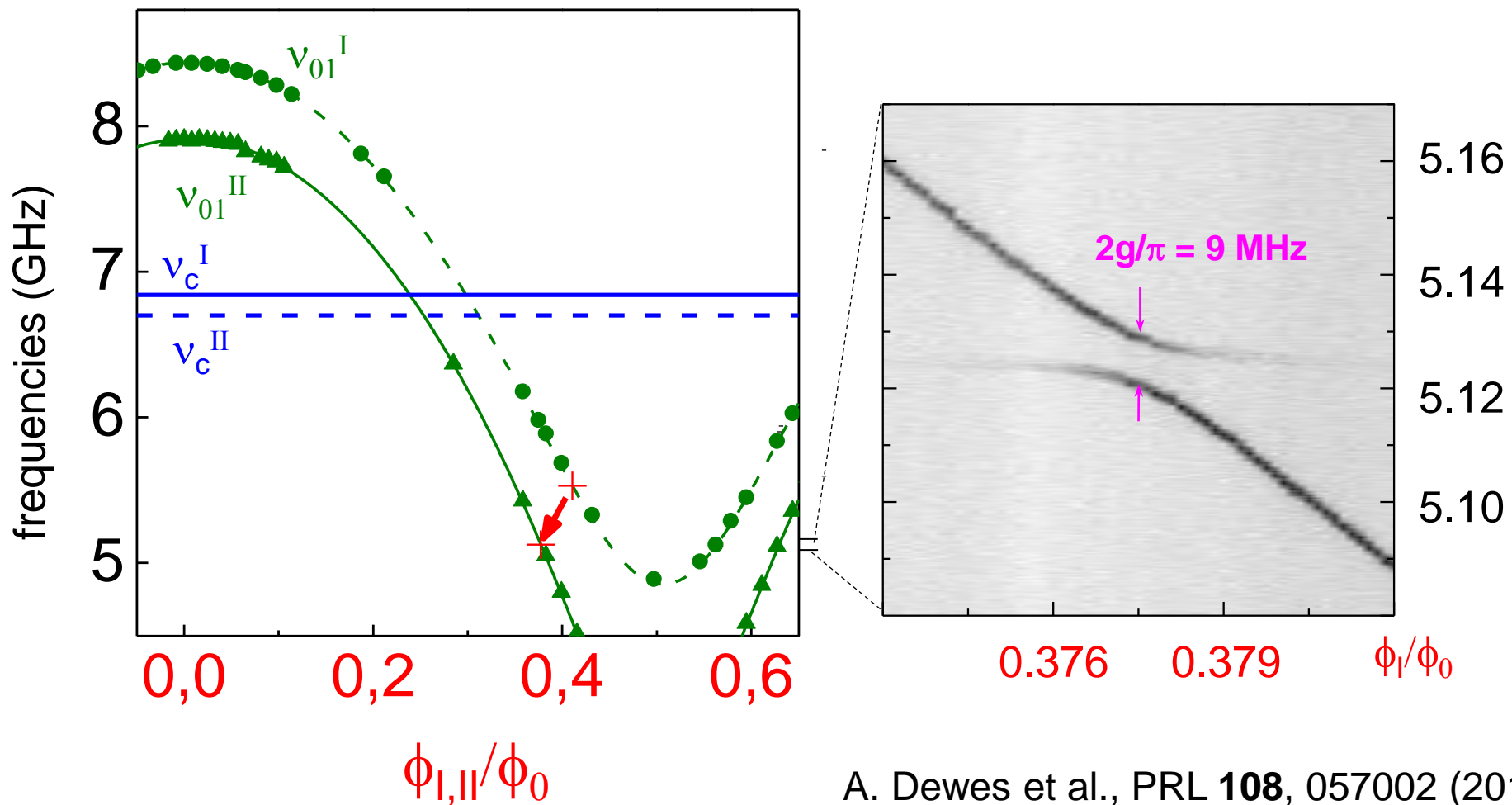
(Saclay, 2011)



Example : capacitively coupled transmons with individual readout

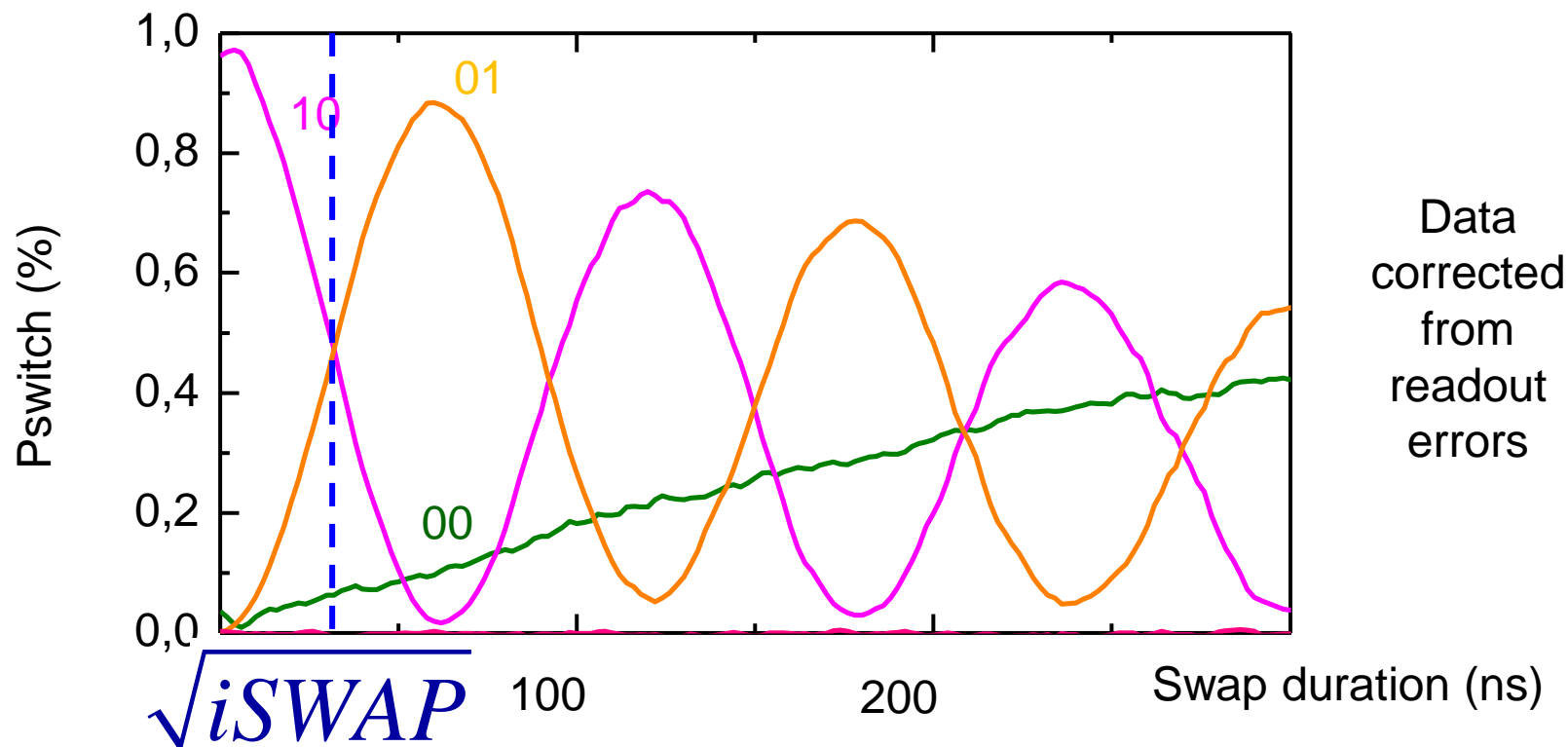
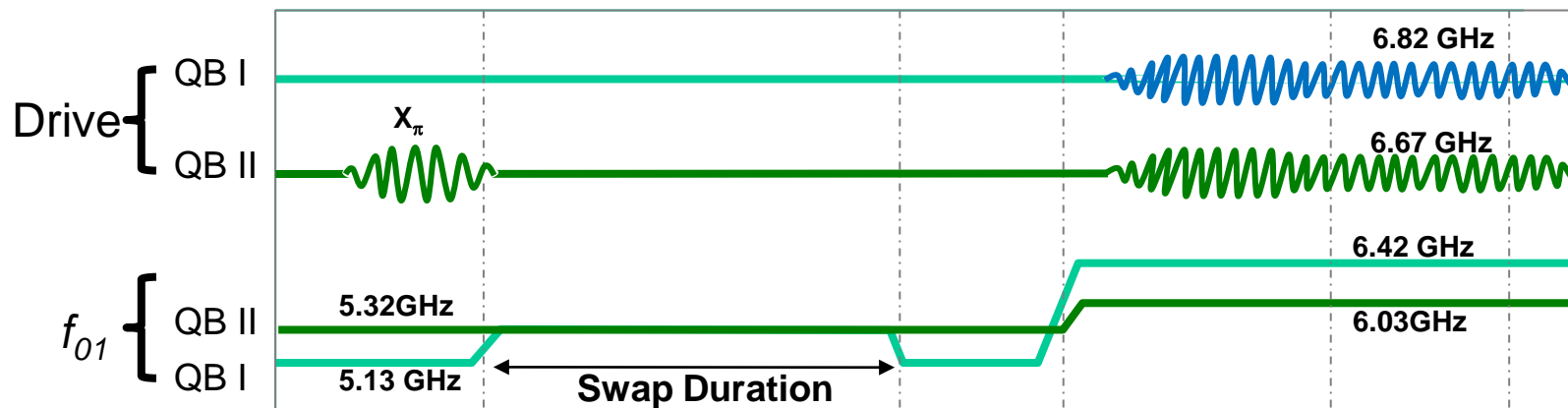


Spectroscopy of the qubit-qubit interaction

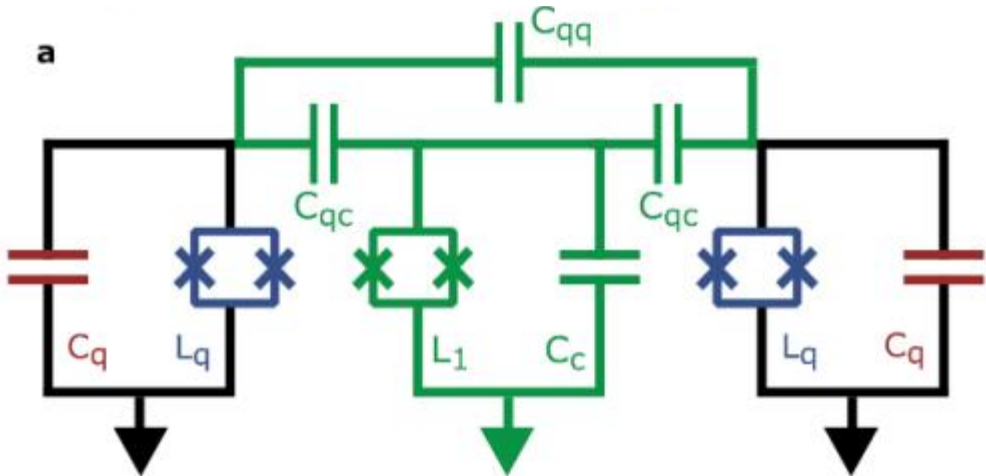


A. Dewes et al., PRL 108, 057002 (2012)

SWAP between two transmon qubits

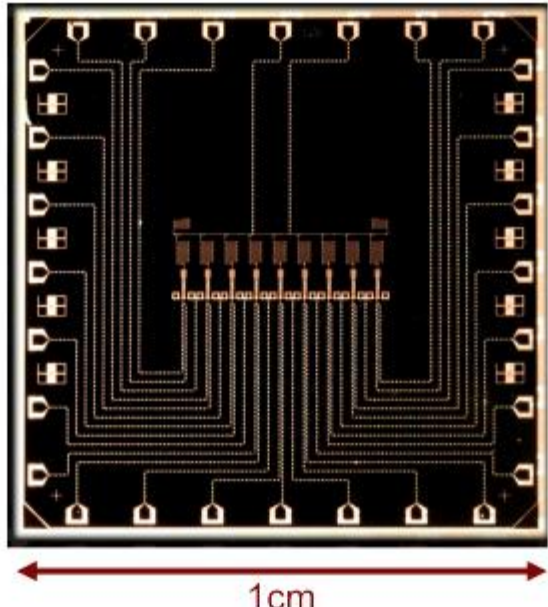


Capacitive Coupling between two qubits

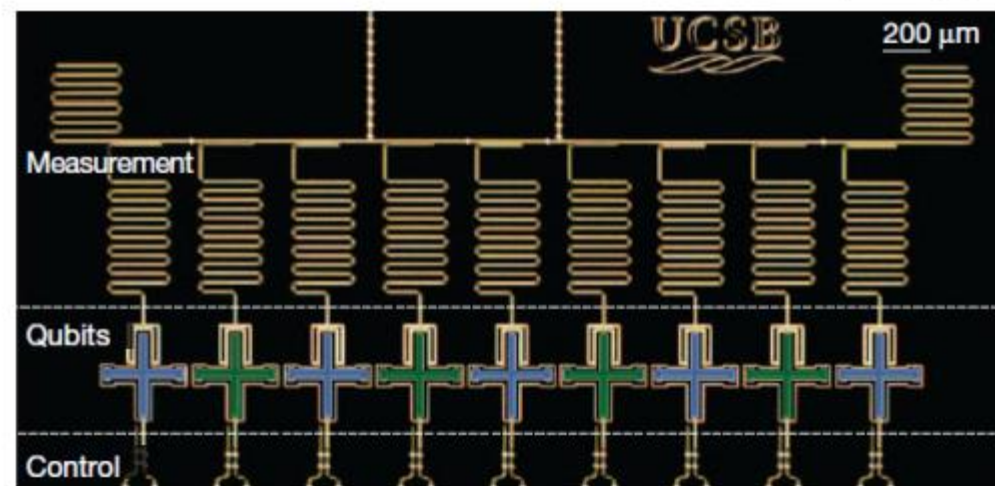


Charles Neill, PhD thesis UCSB (2017)

9 coupled qubits

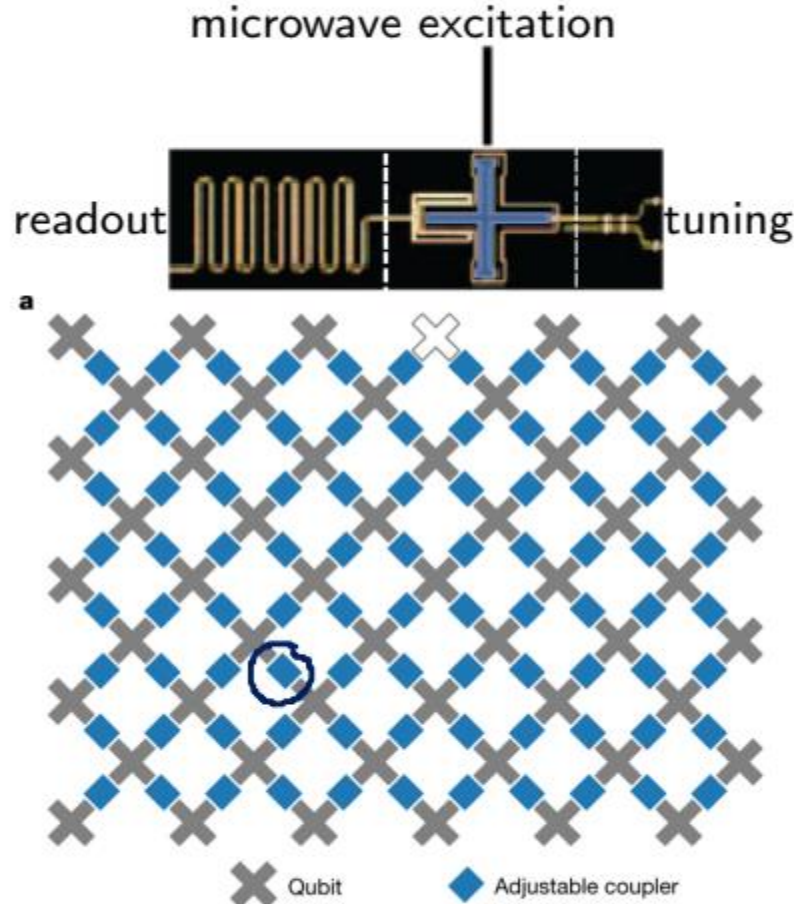


- ▶ direct capacitive coupling between two qubits:
$$H_{\text{int}} = \frac{\hat{Q}_1 \hat{Q}_2}{C_{\text{eff}}} = \hbar g (a_1^\dagger a_2 + a_2^\dagger a_1)$$
- ▶
$$g = \frac{C_{qq}}{\sqrt{C_1 C_2}} \frac{\sqrt{\omega_1 \omega_2}}{2}$$
- ▶ with an intermediate qubit as coupler:
second order tunable coupling



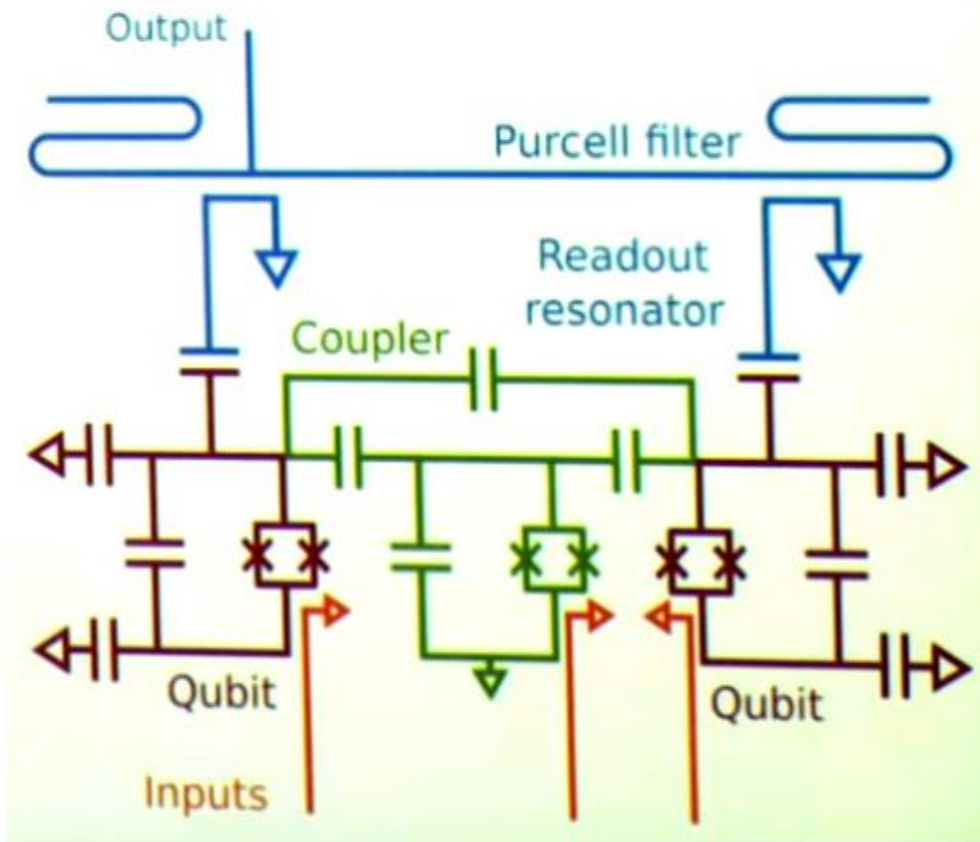
Tunable Capacitive Coupling

Google's Sycamore processor
typical qubit architecture:



Google/Martinis (2019)

scheme for tunable g

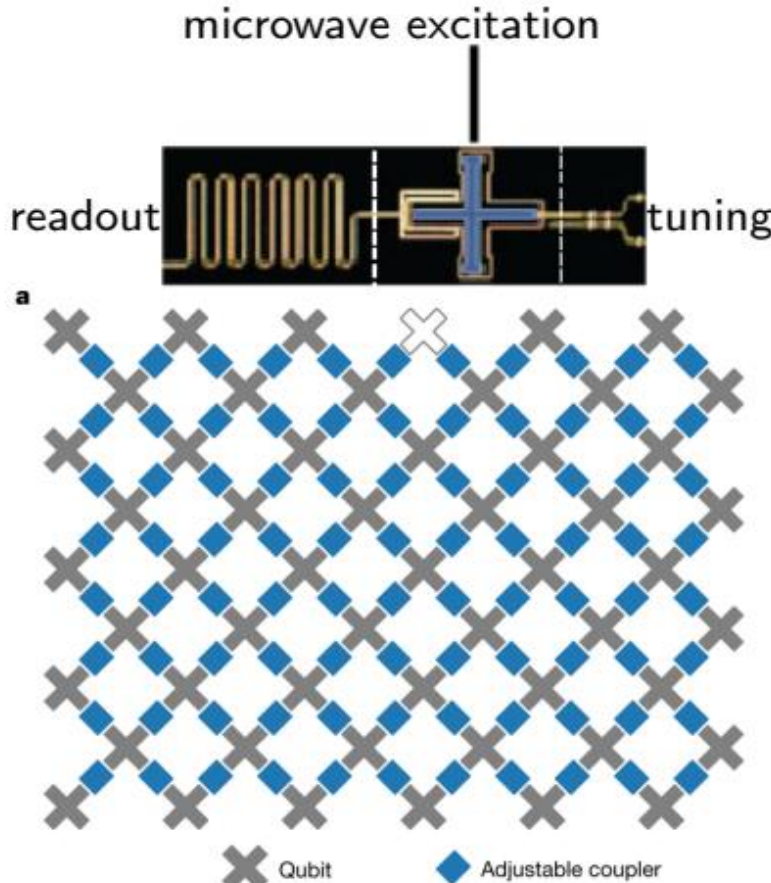


[J. Martini's talk at Caltech, Nov. 2019]

Tunable Capacitive Coupling

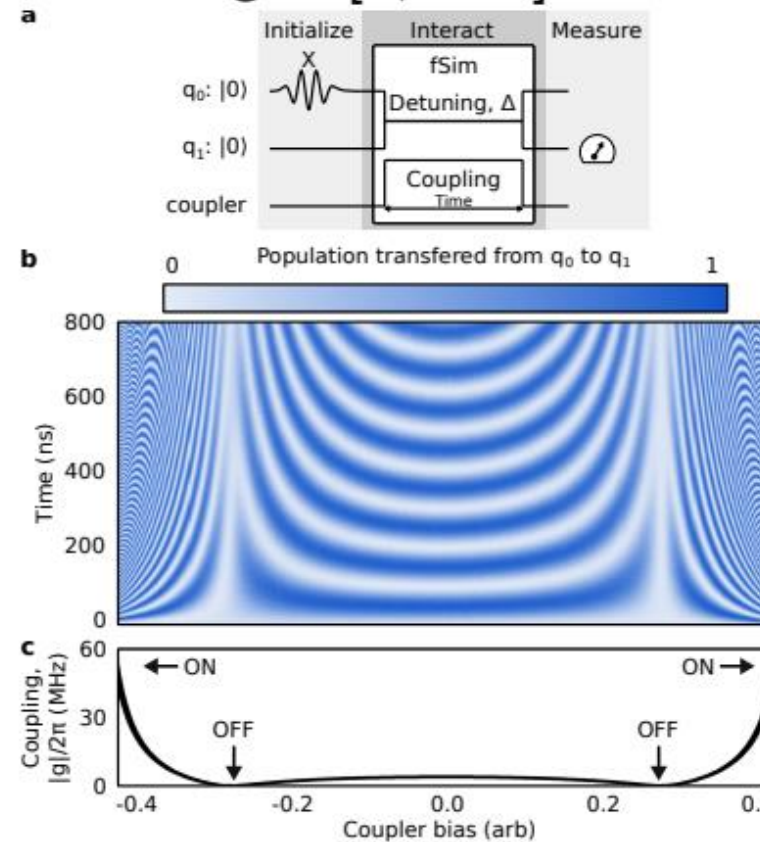
Google's Sycamore processor

typical qubit architecture:



Google/Martinis (2019)

tunable $g \in [5, -40]$ MHz

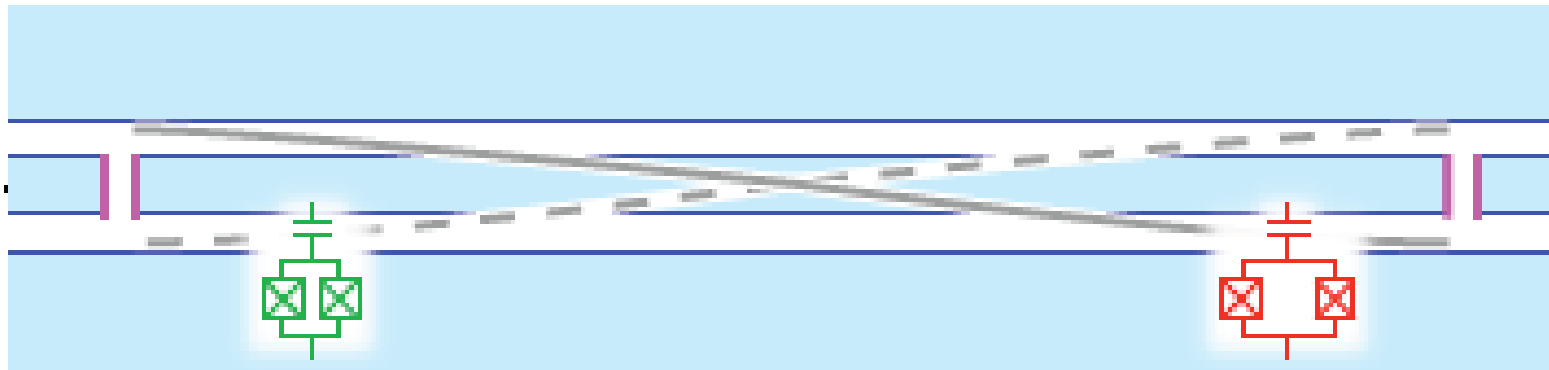


Typical errors:

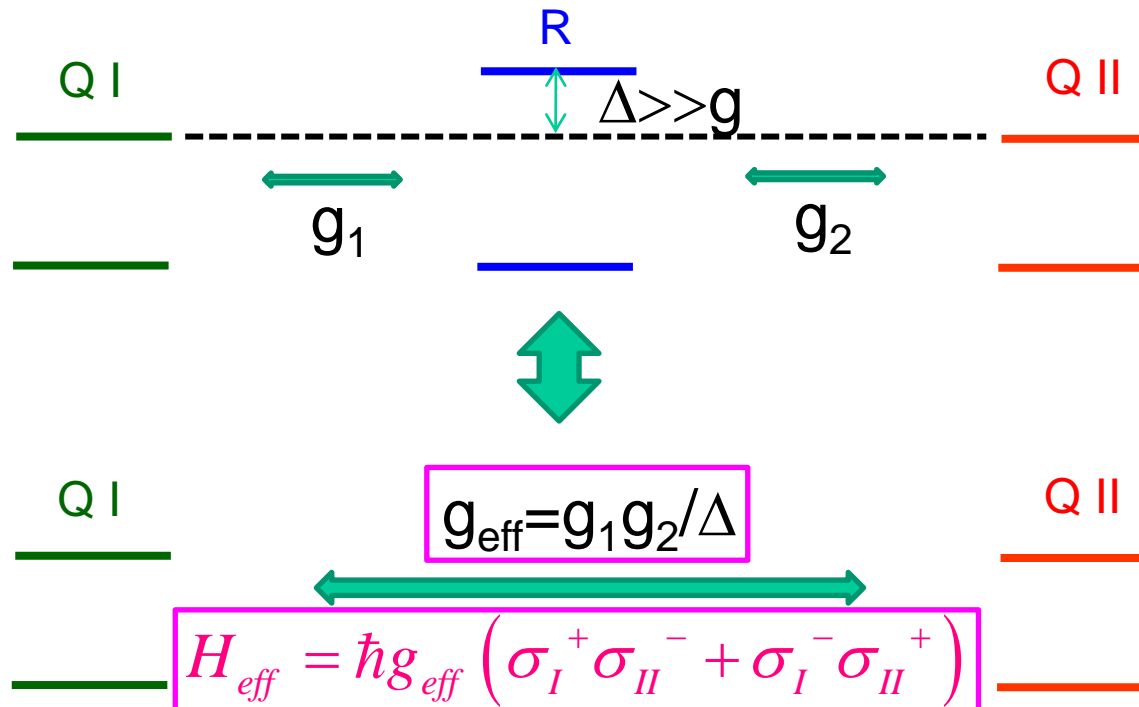
- ▶ 1-qubit gate $\sim 0.2\%$
- ▶ 2-qubit gate $\sim 0.2\text{--}0.9\%$
- ▶ readout $\sim 2\text{--}5\%$

Coupling strategies

2) Cavity mediated qubit-qubit coupling



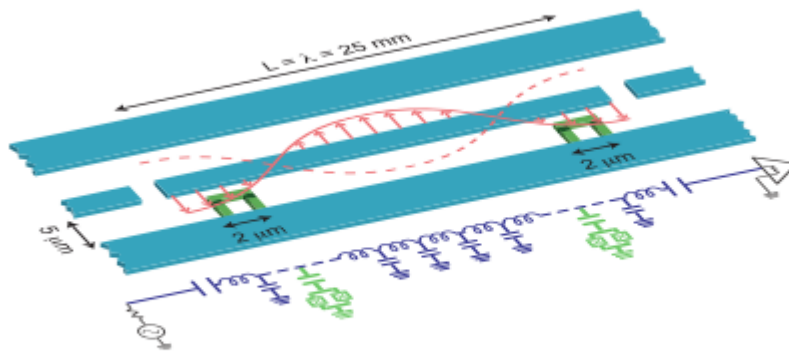
J. Majer et al., Nature 449, 443 (2007)



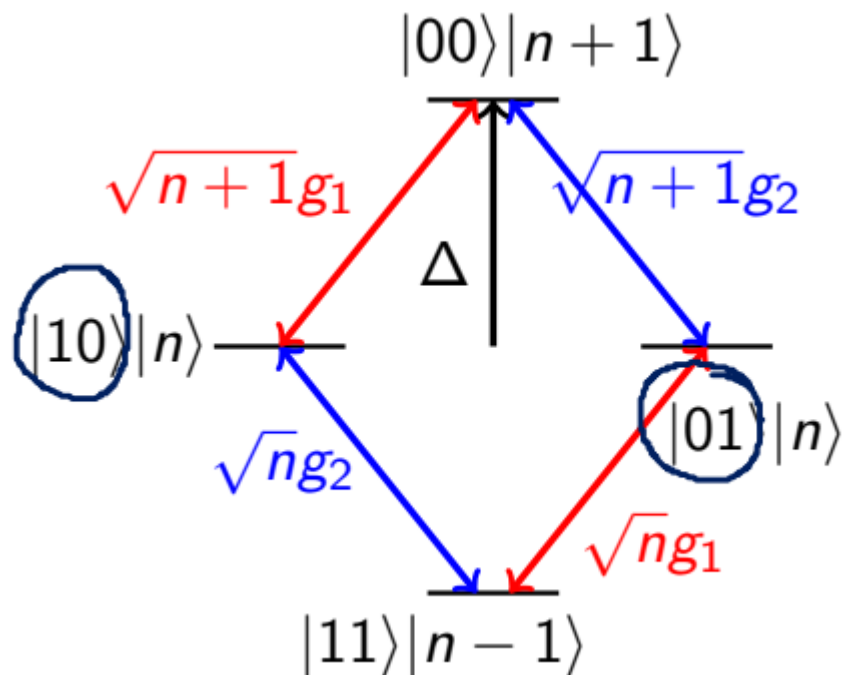
courtesy CEA Saclay

Coupling strategies

2) Cavity mediated qubit-qubit coupling



Blais et al., PRA 75, 032329 (2007)



General idea:

- ▶ insert two qubits in the resonator
- ▶ coupling between qubits mediated by field
- ▶ Two qubits with frequency ω_0
- ▶ Cavity detuned by $\Delta = \omega_c - \omega_0$
- ▶ Effective coupling $\hbar g_{\text{eff}}(a_1^\dagger a_2 + a_2^\dagger a_1)$

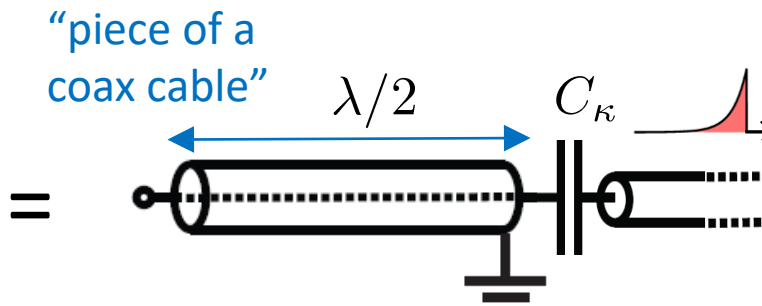
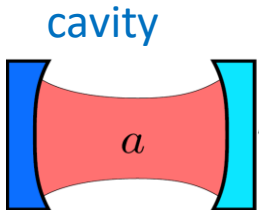
$$g_{\text{eff}} = \frac{(n+1)g_1g_2}{\Delta} + \frac{ng_1g_2}{-\Delta} = \frac{\color{red}{g_1g_2}}{\Delta}$$

- ▶ Coupling turned off when qubits are detuned

Circuit QED architecture

Brief Summary

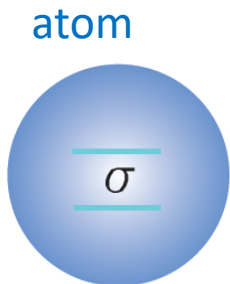
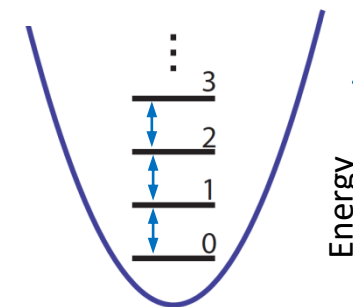
Circuit QED components



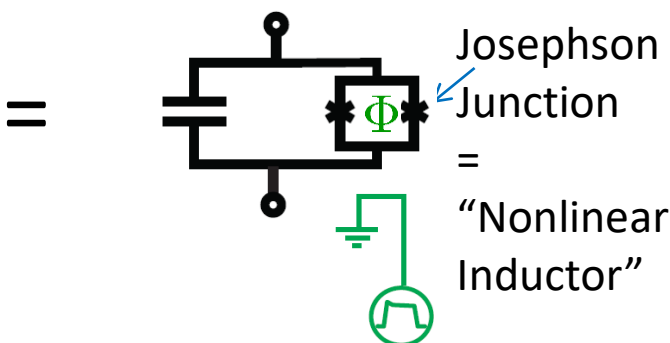
Radiation field stored inside:

$$H = \hbar\omega a^\dagger a$$

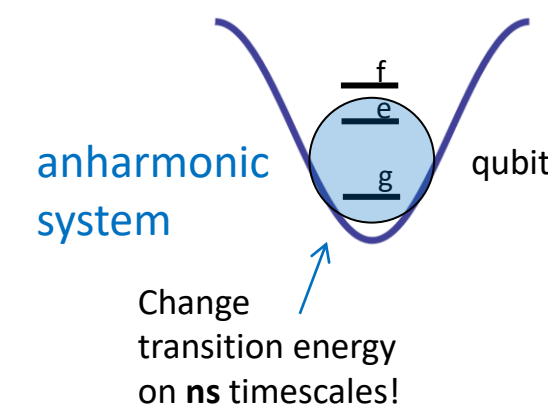
harmonic oscillators



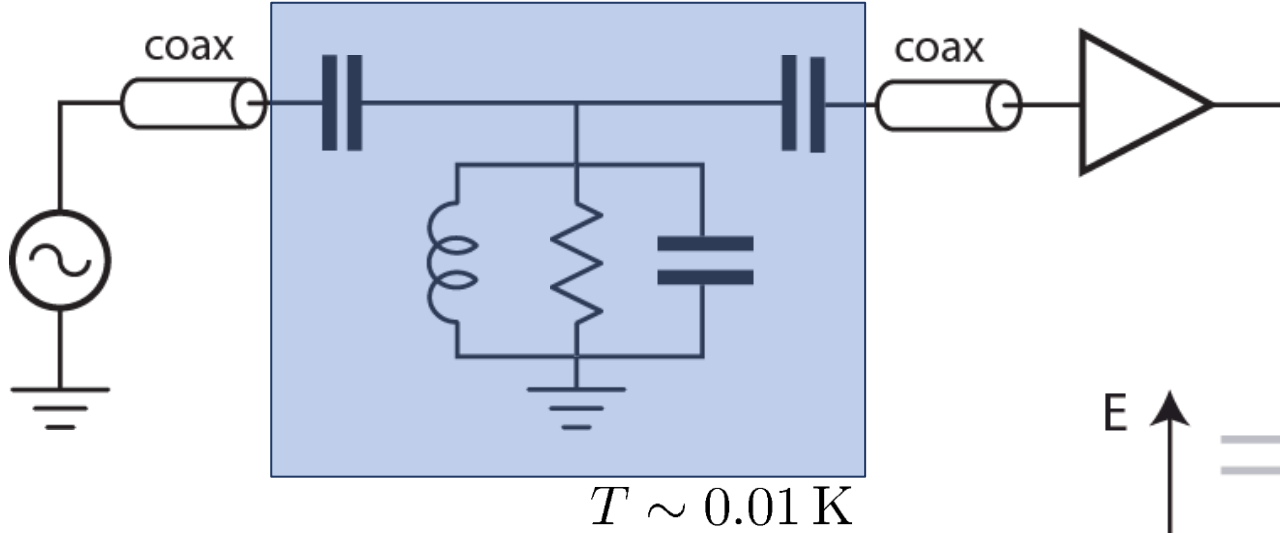
transmon



Josephson Junction
= "Nonlinear Inductor"



How to Operate Circuits Quantum Mechanically?



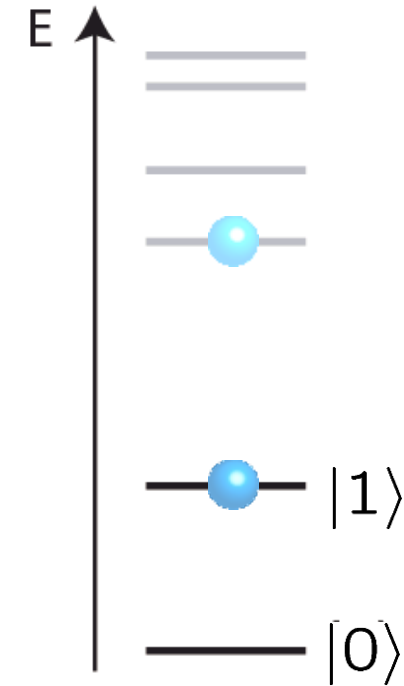
recipe:

avoid dissipation

work at low temperatures

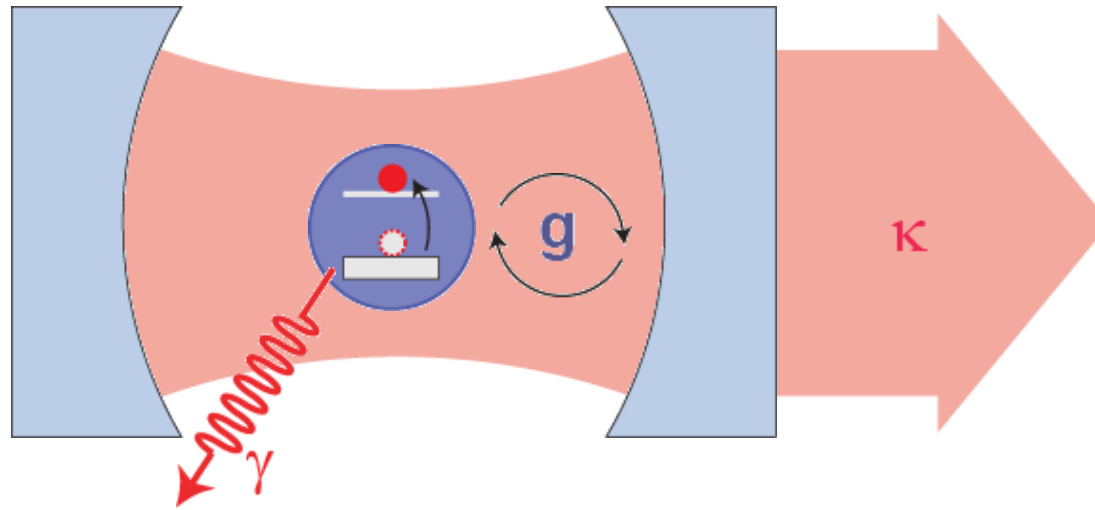
isolate quantum circuit from environment

Can one actually build and operate such circuits?



Circuit Quantum Electrodynamics

interaction of **atom** and **photon** in a cavity



Jaynes-Cummings Hamiltonian

$$H = \boxed{\hbar\omega_r \left(a^\dagger a + \frac{1}{2} \right)} + \boxed{\frac{\hbar\omega_a}{2} \sigma^z} + \boxed{\hbar g(a^\dagger \sigma^- + a \sigma^+)} + H_\kappa + H_\gamma$$

quantized resonator field qubit coupling

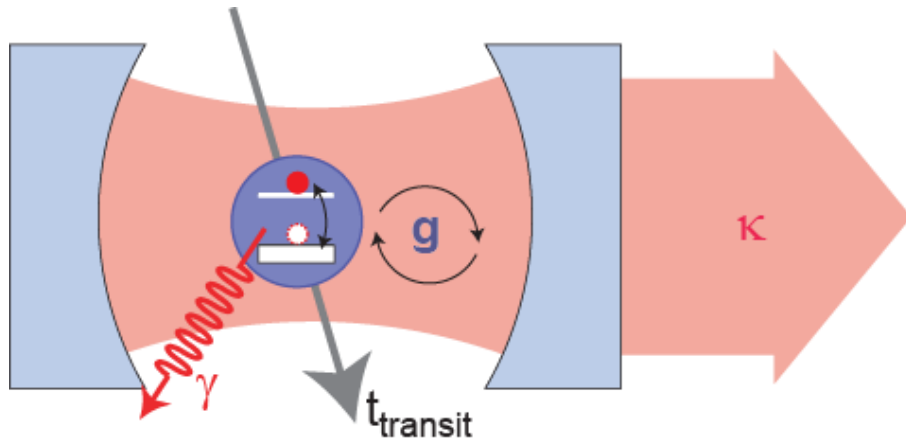
strong coupling limit:

$$g = dE_0/\hbar > \gamma, \kappa, 1/t_{\text{transit}}$$

D. Walls, G. Milburn, Quantum Optics, Springer-Verlag, Berlin (1994)

S. Haroche & J. Raimond, Exploring the Quantum, OUP Oxford (2006)

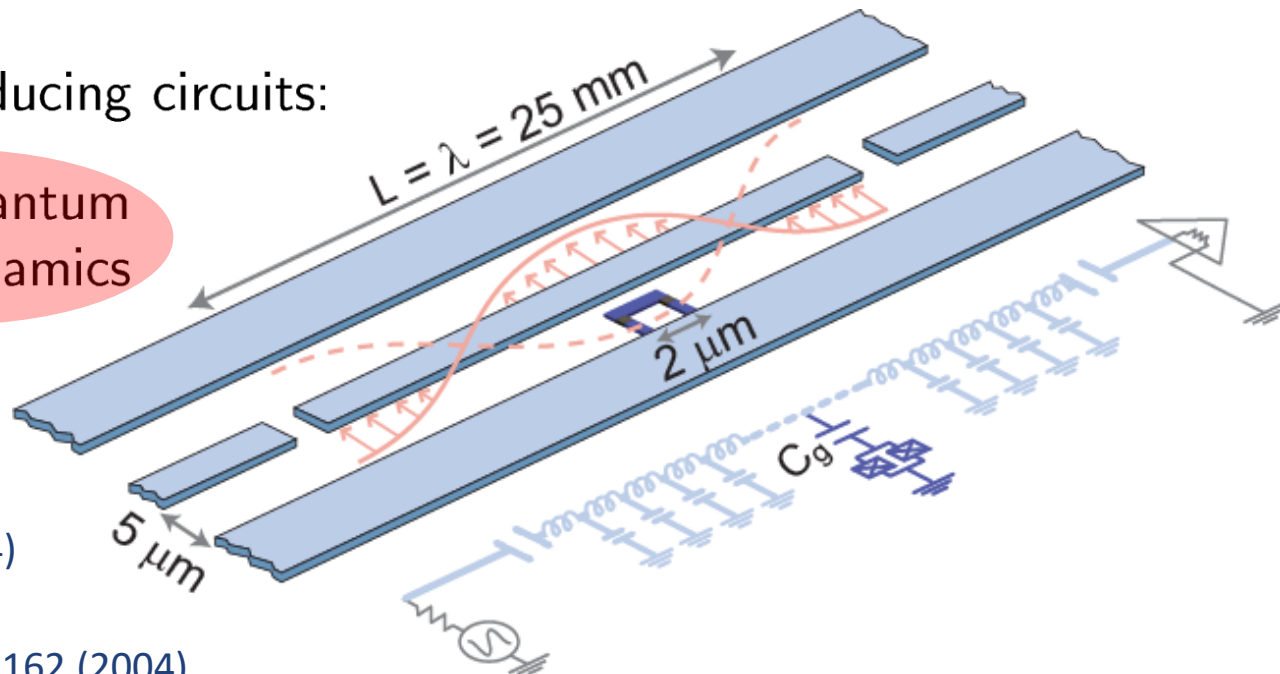
First Cavity QED Experiments with Superconducting Circuits



Controllable coherent interaction of single photons with individual two level systems (qubits)

... in superconducting circuits:

circuit quantum
electrodynamics



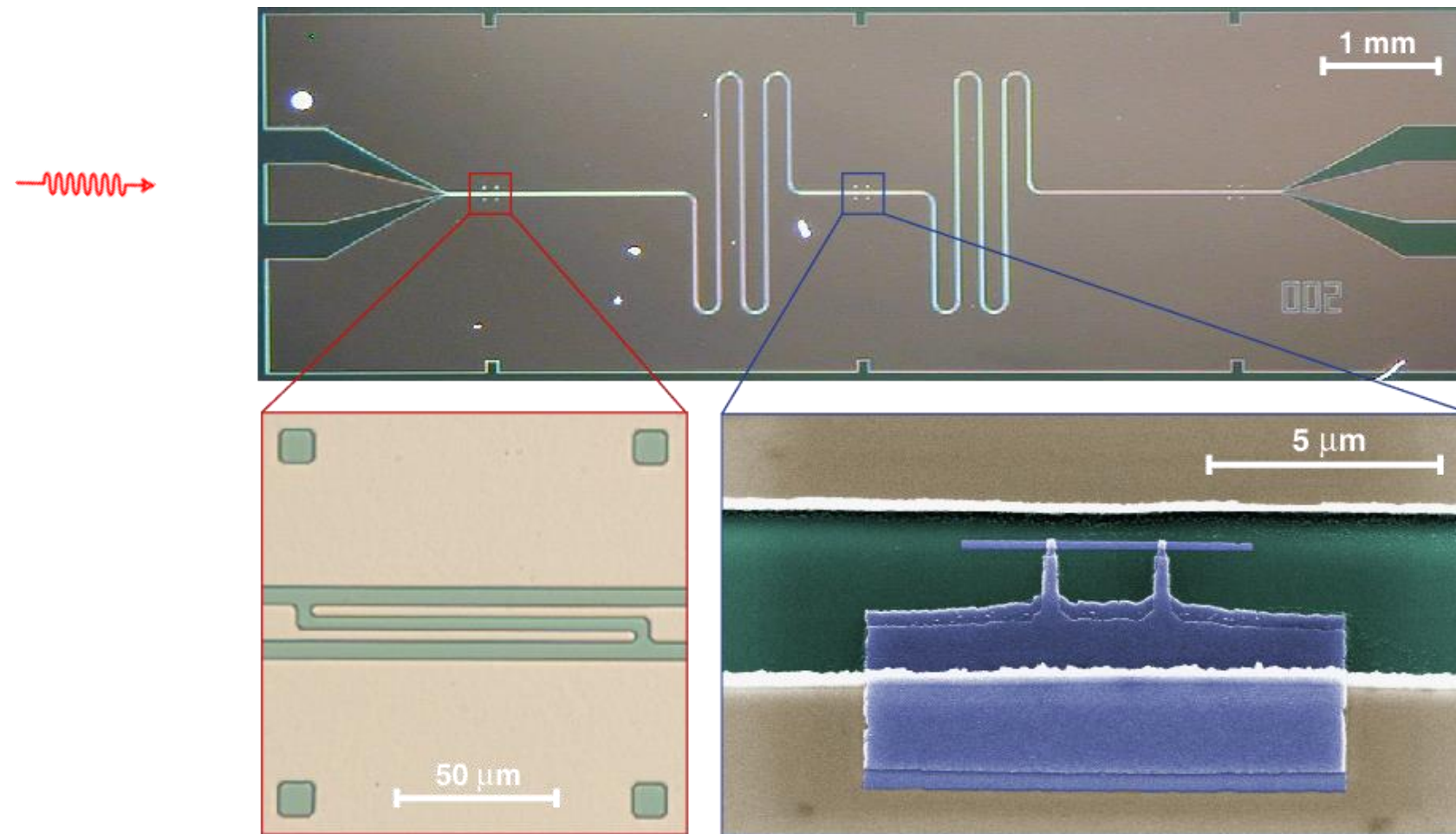
A. Blais, et al.,
PRA **69**, 062320 (2004)

A. Wallraff et al.,
Nature (London) **431**, 162 (2004)

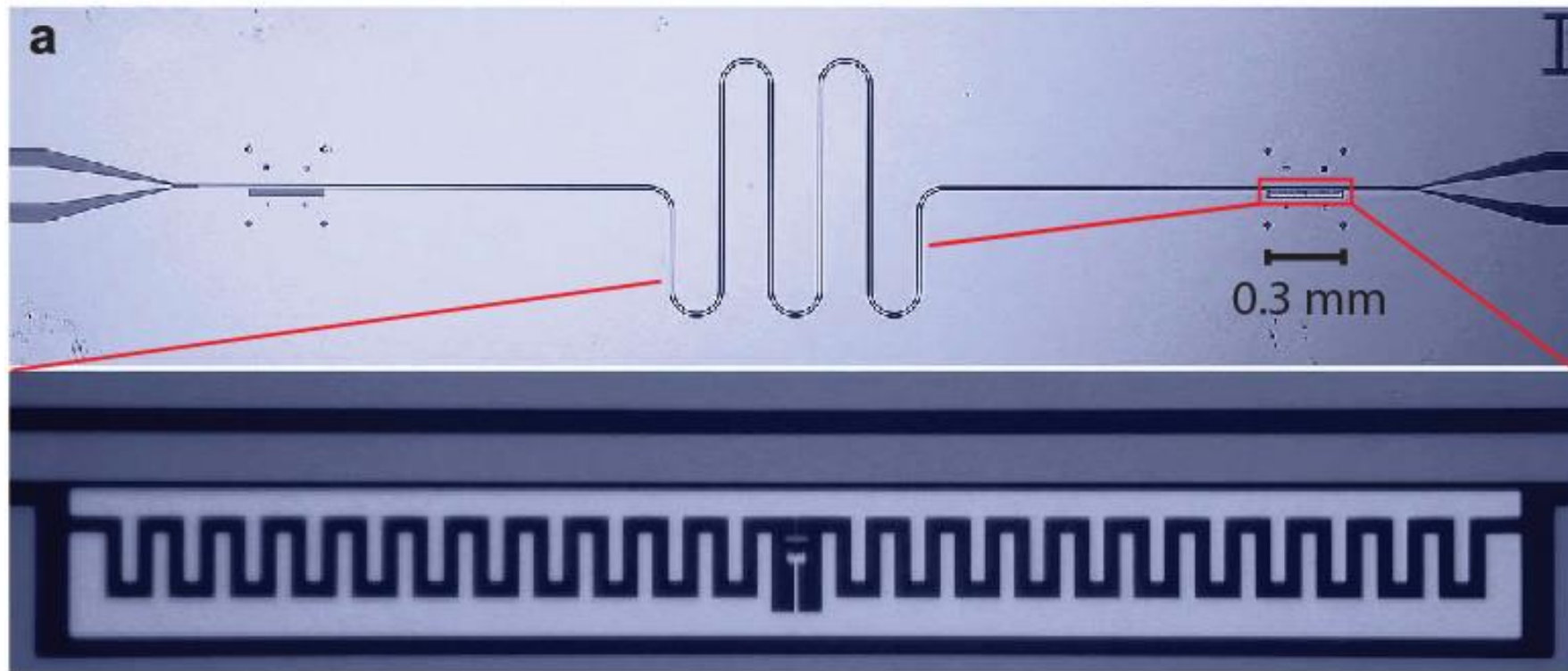
Elements:

- the cavity: a superconducting 1D transmission line resonator with **large vacuum field E_0** and **long photon life time $1/\kappa$**
- the artificial atom: a superconducting qubit with **large dipole moment d** and **long coherence time $1/\gamma$**

The First Superconducting Cavity QED Circuit

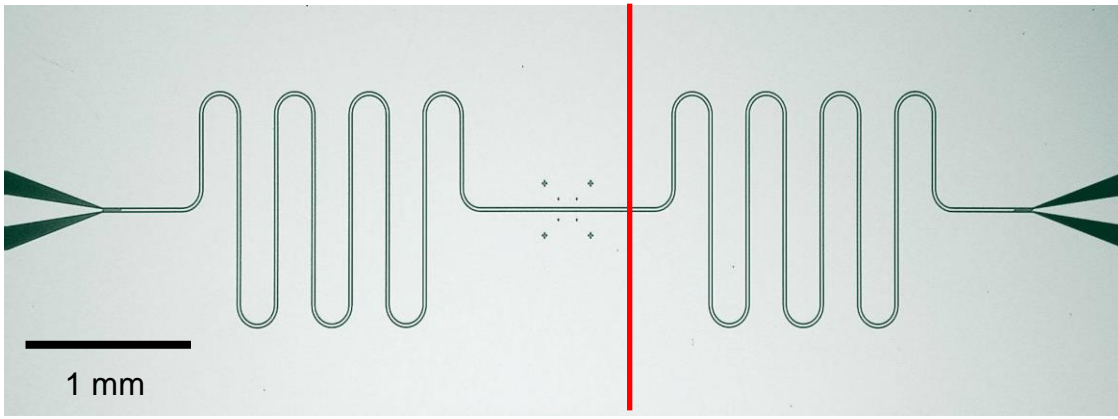


Realization with a Transmon

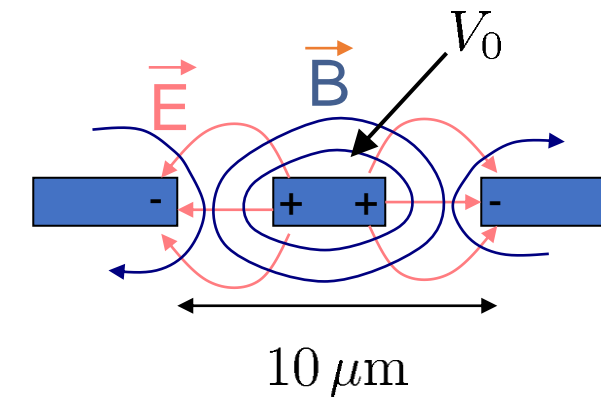


L. Frunzio et al., IEEE Trans. on Appl. Supercon. **15**, 860 (2005)

Vacuum Field in 1D Cavity



cross-section
of transm. line (TEM mode):



voltage across resonator in vacuum state ($n = 0$)

$$V_{0,\text{rms}} = \sqrt{\frac{\hbar\omega_r}{2C}} \approx 1 \mu\text{V}$$

harmonic oscillator

$$H_r = \hbar\omega_r \left(a^\dagger a + \frac{1}{2} \right)$$

$$E_0 = \frac{V_{0,\text{rms}}}{b} \approx 0.2 \text{ V/m}$$

for $\omega_r/2\pi \approx 6 \text{ GHz}$ ($C \sim 1 \text{ pF}$), $b \approx 5 \mu\text{m}$

$\times 10^6$ larger than E_0
in 3D microwave cavity

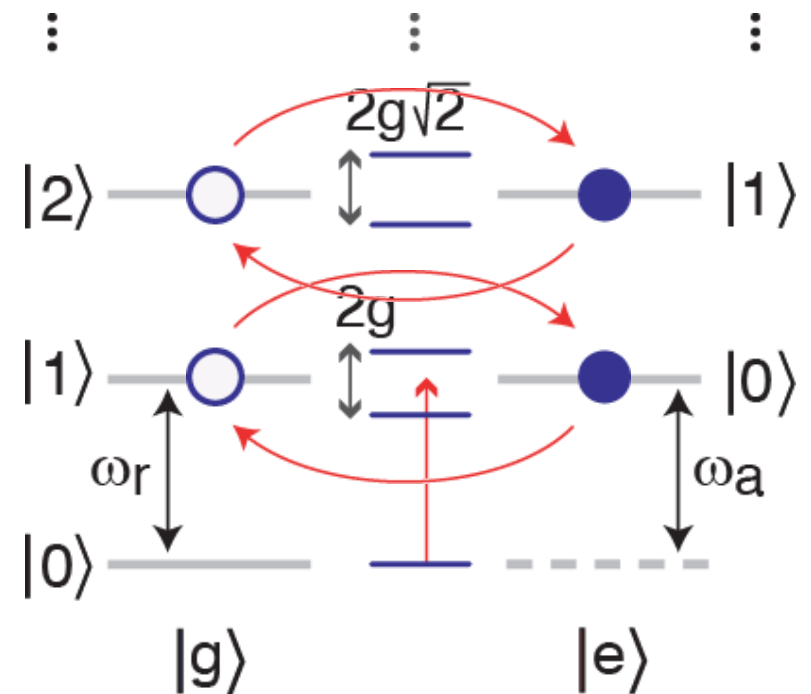
Dressed States Energy Level Diagram

$$H = \hbar\omega_r \left(a^\dagger a + \frac{1}{2} \right) + \frac{\hbar\omega_a}{2} \sigma^z + \hbar g(a^\dagger \sigma^- + a \sigma^+)$$

A. Blais, et al., *PRA* **69**, 062320 (2004)

on resonance: $\omega_a - \omega_r = \Delta = 0$

strong coupling limit: $g = \frac{dE_0}{\hbar} > \gamma, \kappa$



Jaynes-Cummings Ladder

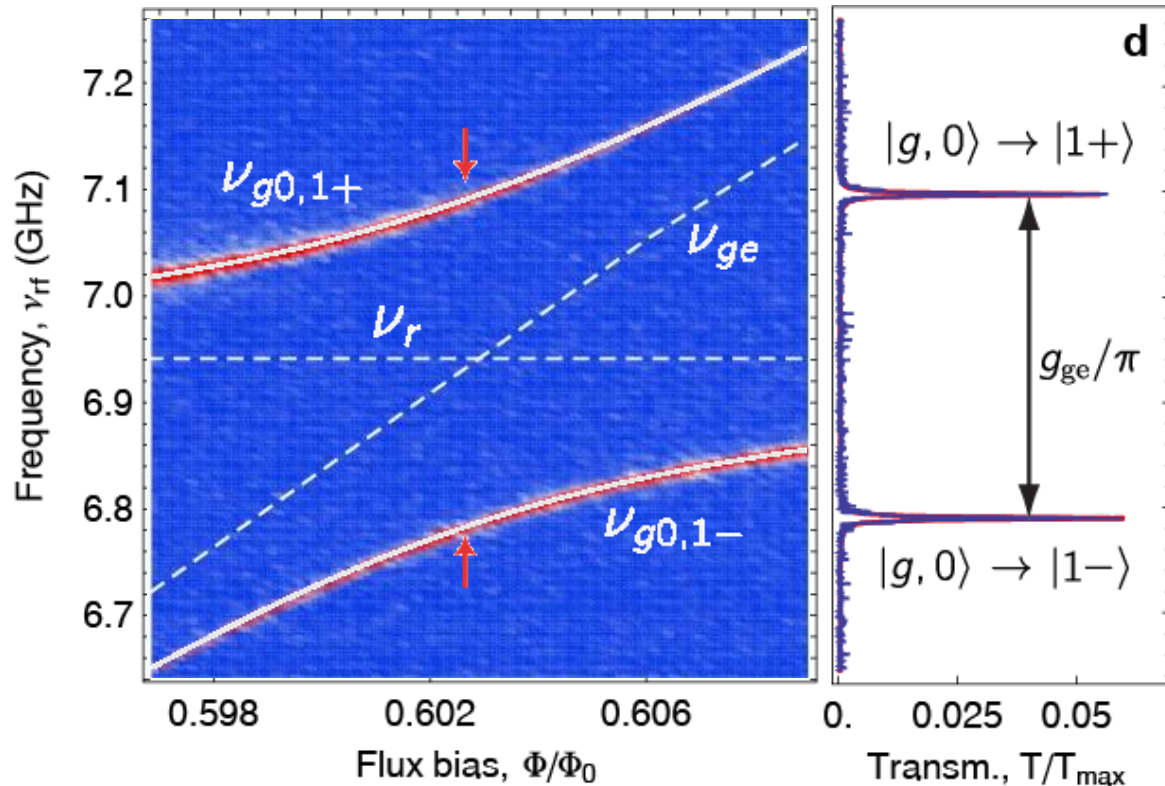
atomic cavity QED reviews:

J. Ye., H. J. Kimble, H. Katori, *Science* **320**, 1734-1738 (2008)

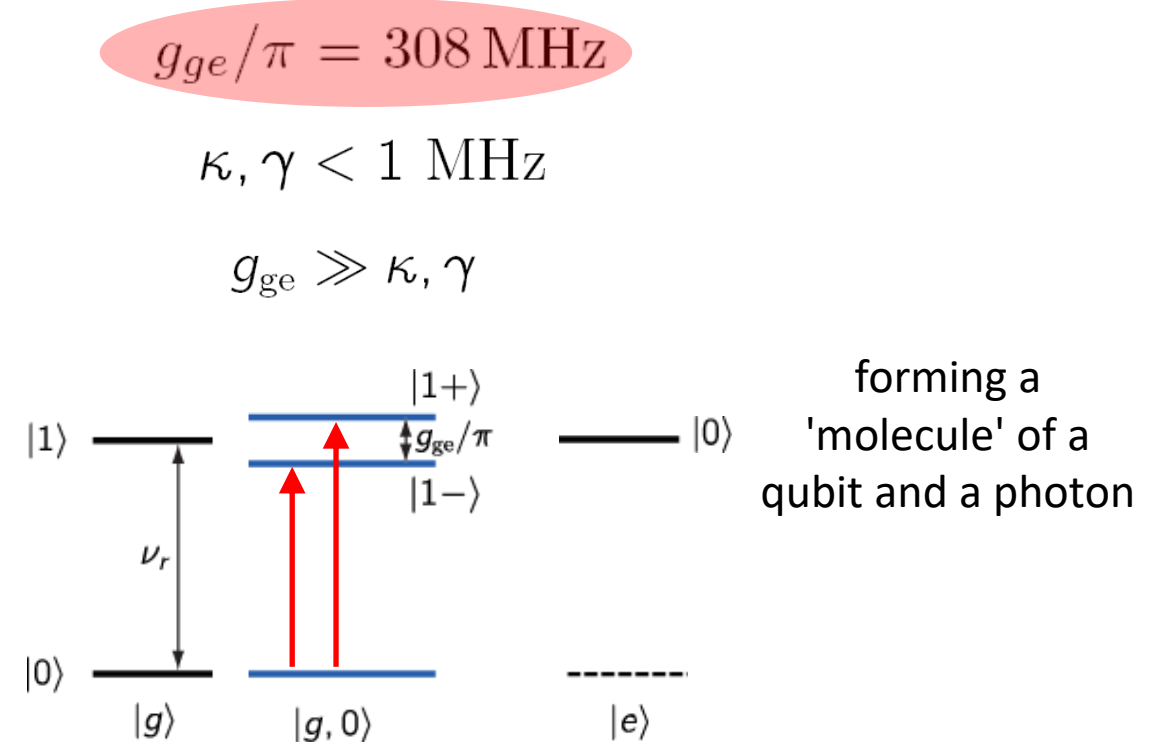
S. Haroche & J. Raimond, *Exploring the Quantum*, OUP Oxford (2006)

Resonant Vacuum Rabi Mode Splitting

Measured with one photon ($n=1$):



very strong coupling:



first demonstration in a solid: A. Wallraff et al., *Nature (London)* **431**, 162 (2004)

this data: J. Fink et al., *Nature (London)* **454**, 315 (2008)

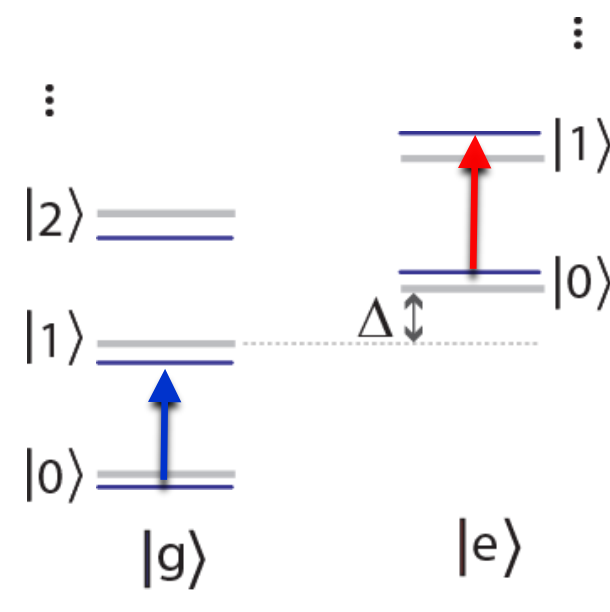
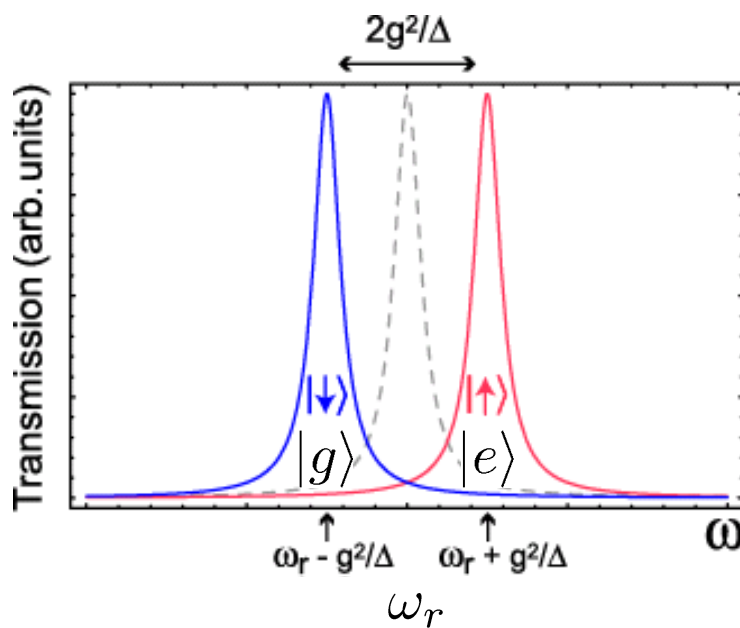
R. J. Schoelkopf, S. M. Girvin, *Nature (London)* **451**, 664 (2008)

Non-Resonant (Dispersive) Interaction

approximate diagonalization for $|\Delta| = |\omega_a - \omega_r| \gg g$

$$H \approx \hbar \left(\omega_r + \frac{g^2}{\Delta} \sigma_z \right) a^\dagger a + \frac{1}{2} \hbar \left(\omega_a + \frac{g^2}{\Delta} \right) \sigma_z$$

//
cavity frequency shift



qubit detuned by Δ
from resonator

- A. Blais *et al.*, PRA 69, 062320 (2004)
A. Wallraff *et al.*, Nature (London) 431, 162 (2004)
D. I. Schuster *et al.*, Phys. Rev. Lett. 94, 123062 (2005)
A. Fragner *et al.*, Science 322, 1357 (2008)

Non-Resonant Qubit-Photon Interaction

approximate diagonalization in the dispersive limit $|\Delta| = |\omega_a - \omega_r| \gg g$

$$H \approx \hbar \left(\omega_r + \frac{g^2}{\Delta} \sigma_z \right) a^\dagger a + \frac{1}{2} \hbar \left(\omega_a + \frac{g^2}{\Delta} \right) \sigma_z$$

//
cavity frequency shift
and qubit ac-Stark shift

